Tanzania Journal of Science
Volume 51(4), 2025
journal homepage: https://commons.udsm.ac.tz/tjs/

Modelling the impact of multiple control strategies on the spread of phyllody disease in sesame

Furaha M Chuma[1] and Augustino I Msigwa[2*]
[1] *Department of Physics, Mathematics, and Informatics, Dar es Salaam University College of Education, P.O. Box 2329, Dar es salaam, Tanzania*
[2] *Department of Mathematics, University of Dar es Salaam, P.O Box 35062, Dar es salaam, Tanzania*
Emails: furaha.chuma@udsm.ac.tz, msigwa.augustino@udsm.ac.tz

Keywords

Phyllody disease;
Phytoplasma;
Biological control;
Chemical control;
Roguing

Abstract

Phyllody disease, caused by phytoplasma and transmitted by insect vectors such as leafhoppers, poses a serious threat to the productivity of sesame (Sesamum indicum) as it has caused substantial yield and oil-quality losses worldwide, with documented seed-yield reductions ranging from 38% to as high as 80% in severe outbreaks, particularly in Africa and India. Understanding phyllody dynamics is therefore critical to safeguard yields and trade. While some modeling efforts exist for sesame phyllody (for example, statistical and prediction-focused approaches), mechanistic transmission models (SEIR) assessing its full impact remain scarce. This study therefore develops and analyses impact of multiple control strategies on the control of Phyllody disease in Sesame using a deterministic compartmental mode. The model incorporates both plant and vector populations, subdivided into susceptible and infected classes, and integrates multiple control strategies; biological measures such as crop rotation and resistant seeds, chemical interventions targeting both plants and vectors, and roguing of infected plants. The effective reproduction number, R_e, is derived using the next-generation matrix method, providing a threshold for disease spread or elimination. Moreover, the sensitivity analysis shows that the transmission rates from plants to vectors, (φ), and from vectors to plants, (α), are the dominant positive drivers of the effective reproduction number Re; increases in either φ or α raise R_e. In contrast, increasing the roguing rate of infected plants, (τ), and intensifying chemical applications against leafhoppers, (ν), substantially reduce R_e, indicating that stronger plant removal and vector control measures are especially effective at lowering transmission Numerical simulations demonstrate that chemical control and biological interventions significantly reduce disease prevalence, particularly when combined with roguing. The findings underscore the importance of integrated management, as roguing alone is insufficient to halt disease spread. The model offers a valuable tool for guiding sustainable strategies to protect sesame crops from phyllody disease.

2000 MR Subject Classification: 92B05, 92D30, 93A30

Introduction

Sesame is an important oilseed crop in the world grown for food and commercial purposes particularly in Asia and Africa (Abdipour et al. 2018, Gupta et al. 2018, Baath et al. 2022, Lukurugu et al. 2023). Africa and Asia continents contribute 95.5% of the world's total sesame production while America and Europe contribute only 4.1% of the total production worldwide (Lukurugu et al. 2023). The top ten countries producing sesame seeds in the world include Sudan, Myanmar, Tanzania, India, Nigeria, China mainland, Burkina Faso, Chad, Ethiopia and Southern Sudan (Lukurugu et al. 2023). The crop products are mainly used for cooking, manufacturing medicines and cosmetic, and additional of food supplements. Sesame oil is primarily composed of oleic, linoleic, palmitic, and stearic fatty acids (Baath et al. 2022, Gupta et.al 2022).

Sesame yields are suffering from many diseases including the Phyllody (Gupta et al. 2018, Kolte 2018, Vamshi et al. 2018, Verma et al. 2025). Phyllody is serious disease of sesame caused by phytoplasma affecting the leaves of the plant (Vamshi et al. 2018). The disease tends to be more severe in areas with warm temperatures, particularly in regions with temperature above 250C, high relative humidity (above 90% per cent) and prolonged high rainfall (El-Mashharawi and Abu-Naser 2019). The disease has caused substantial yield and oil-quality losses worldwide, with documented seed-yield reductions ranging from ~38% to as high as 80% in severe outbreaks (Ikten et al. 2016, Ahmed et al. 2022).

The disease symptoms may vary with the phytoplasma, post plant, stage of the disease, age of the plants at the time of infection and environmental condition (Gupta et .al 2022). The disease symptoms include stunted growth, shortened internodes, and the proliferation of small,

*Corresponding author: msigwa.augustino@udsm.ac.tz
Received 1 July 2025; Revised 12 Nov 2025; Accepted 22 December; Published 29 December 2029
https://doi.org/10.65085/2507-7961.1115

ISSN 0856-1761, e-ISSN 2507-7961

narrow leaves. Infection may also be seen on flowers and capsules of the plant whereby infected capsules are always poorly developed with shriveled seeds (Kolte 2018, Gupta et.al 2022, Verma et al. 2025).

Different control strategies are occasionally applied for rescuing the sesame production at individual and large-scale farming. The strategies can include both biological and chemical controls and can be applied at different stages of the crop growth. For example, seeds treatment such as *Trichoderma harzianum* can be applied to seeds before planting to enhance protection and growth (Kumari et al. 2016, Gupta et. al 2022, Singh et al. 2022, Boopathi et al. 2023, Yadav et al. 2023, Chouksey et al.2025). Other biological treatments like *Arbuscular mycorrhizal* fungi and plant growth-promoting rhizobacteria can be applied to the soil around the sesame plants. These help to improve soil fertility, enhance plant growth, and reduce the incidence of the phyllody disease (Singh et al. 2020, Ransingh et al. 2021, Boopathi et al. 2023). In addition, cultural practices like crop rotation, plant of resistant varieties, and roguing of infected plants and disposing them properly can help to control the spread of the phyllody disease to nearby healthy plants (Kumari et al. 2016, Singh et al. 2020, Gupta et .al 2022, Boopathi et al. 2023).

Disease life Cycle

The phyllody disease of sesame is caused by *phytoplasma*, a type of bacteria-like organism that infect plants through feeding of insect vectors, such as leafhoppers, planthoppers, and psyllids (Gupta et. al 2022, Santha Lakshmi Prasad et al. 2025). The *phytoplasma* inters the plant through the mouth parts of the insect and moves to the phloem tissues where it multiplies and spreads. After infection, the bacteria incubate within the plant for several weeks, typically two to six weeks, before clinical symptoms of the disease become visible (Ransingh et al. 2021). After the incubation period, the infected plant begins to show symptoms such as stunted growth, shortened internodes, and the proliferation of small, narrow leaves (Boopathi et al. 2023). As the disease progresses, the plant's flowers become distorted, with stunted or missing reproductive structures and the formation of green, leaf-like structures in their place. In severe cases, the infected plant may not produce visible seeds, or the seeds themselves may be infected with phytoplasma bacteria, leading to further spread of the disease. During the plant's dormant phase, the bacteria may remain in the plant tissues or in the soil, ready to infect new plants in the next growing season. Mathematical models have recently been useful tools for understanding the dynamics of plant diseases. In particular, various studies have been conducted on plant disease transmission (Shi et al. 2014, Al Basir et al. 2018, Vamshi et al. 2018, Kolte SJ 2018, Gupta et al. 2018, Chapwanya and Dumont 2021, Stella et al. 2021, Gupta et .al 2022, Mrope 2025a, Mrope 2025b, Verma et al. 2025).

Al Bashir et al. 2018 studied the effects of awareness-based interactions on the transmission of mosaic disease of Jatropha in cassava plantations. Al Basir et al. 2018, and Alemneh et al. 2019 proposed a vector-borne plant disease model to investigate the role of vectors in the spread of plant diseases. Stella et al. 2021, developed a nonlinear mathematical model on the dynamics of plant diseases in the presence of predators. In this model, two-time delays were considered. Al Basir et al. 2018, examined the effects of incubation delay and the latent period on the dynamics of plant diseases. Chapwanya and Dumont 2021, investigated the interaction between crops, vectors, and viruses in the transmission dynamics of cassava mosaic disease. Kumar et al. 2022 incorporated equal dimensionality and memory effects into their model to analyse the infection rate of Beddington-De Angelis fractional responses to vector-borne plant epidemics. Bounkaicha and Allali 2024 studied the global analysis of a spatial-temporal fractional-order SIR infection model with a saturated incidence rate. Fantaye and Birhanu 2023 examined the transmission dynamics of Cotton Leaf Curl Virus disease using fractional-order derivatives. Their study revealed that the disease spreads more slowly as the fractional order decreases from 1.00 to 0.72. Melese et al. 2022 modelled the dynamics of coffee berry disease infestation by considering interactions among coffee berries, vector populations, and fungal pathogens. None of the aforementioned studies develop a mechanistic (compartmental)model for sesame phyllody. Accordingly, we formulate a sesame–phytoplasma-leafhopper transmission model within a plant–vector ODE frameworks applied in the aforementioned studies.

To date, no mechanistic model (SEIR) has yet been proposed specifically for phyllody disease in sesame. To address this gap, a deterministic plant–vector model is developed to quantify how roguing, chemical control, and biological/cultural measures (e.g. crop rotation, early roguing) affect R_e and disease prevalence individually and in combination providing a process-based basis for optimizing sesame phyllody management.

Materials and Methods

A deterministic plant–vector model for sesame phyllody is formulated in which leafhoppers transmit phytoplasma to healthy plants; plant growth is logistic with a carrying capacity, vector abundance increases via births and immigration, infections are irreversible, and pre-maturity plant removal is neglected (Akhtar et al. 2009, Boopathi et al. 2023)

The model consists of two compartments: sesame plants and the leafhopper population. The sesame plants are divided into healthy plants, $S_P(t)$, $E_p(t)$ is the exposed class (infected but no sign) and unhealthy plants, $I_P(t)$. At any time *t*, the total sesame plant population is given by:

$$(t) = S_P(t) + E_p(t) + I_P(t) \quad (1)$$

The vector population is divided into two groups: healthy leafhoppers, $S_V(t)$ and infected leafhoppers, $I_V(t)$. At any time t, the total vector population is given by:

$$N_V(t) = S_V(t) + I_V(t) \quad (2)$$

Susceptible plants grow logistically at the intrinsic rate *r* with carrying capacity K. They acquire infections from infected leafhoppers at the transmission rate $\alpha(1-\psi)$ where ψ represents biological control measures for

sesame seeds and fields before sowing. The parameter α is the transfer rate of phytoplasma from infected leafhoppers to healthy plants. Furthermore, $(1-\psi)$ *is* the effect of biological control reducing infection probability. Additionally, sesame is an annual maturing in approximately 90–110 days (up to 125–135 days in cooler regions) with end-of-season senescence/harvest the dominant removal (Texas and AgriLife 2007). Thus, we treat non-disease attrition of healthy sesame as a small natural death rate acting during the season, and set $\mu_P = 0.003\ day^{-1}$. The rate of change of the susceptible plant population over time (t) is described by the following nonlinear differential equation:

$$\frac{dS_P}{dt} = rS_P\left(1-\frac{S_P+I_P}{K}\right) - \frac{(1-\psi)\alpha S_P I_V}{N_P} - \mu_P \qquad (3)$$

The compartment E_P represents infected but not yet infectious sesame plants during the latent (incubation) period. Plants enter E_P upon successful vector-to-plant transmission, typically modeled by a standard-incidence term, and leave E_P by progressing to the infectious class I_P at rate κ and are reduced at a natural death rate μ_P. Thus, the dynamics of the exposed plants is given by:

$$\frac{dE_p}{dt} = \frac{(1-\psi)\alpha S_P I_V}{N_P} - (\kappa+\mu_P)E_p$$

Moreover, the infectious plants arise only by progression from E_P at rate κ and die due to natural death at a rate μ_P. Thus, the equation governing the dynamics of infectious sesame plants is given by:

$$\frac{dI_P}{dt} = \kappa E_p - (\rho+\tau+\mu_P)I_P \qquad (4)$$

where ρ and τ represent disease-induced death and the roguing of identified infected plants, respectively. The population of healthy vectors increases due to natural birth and migration into the compartment $S_V(t)$ at the rate ωΛ, where ω is the probability of healthy or unhealthy vectors entering the farm. Vectors acquire the infection at the transmission rate ϕ after feeding on infected sesame plants. Additionally, the susceptible vector population decreases due to chemical application at rate ν and natural mortality at rate δ. The susceptible vector population is governed by the following differential equation:

$$\frac{dS_V}{dt} = \omega\Lambda - \frac{\varphi S_V I_P}{N_V} - (\delta+\nu)S_V \qquad (5)$$

Infections in the vector population increase when infected vectors migrate into the farm at the rate $(1-\omega)$. Furthermore, the infected vector population declines due to chemical application at rate ν,death rate disease induced δ and natural death rate μ_P. Hence, the dynamics of $I_V(t)$ are governed by the following differential equation:

$$\frac{dI_V}{dt} = (1-\omega)\Lambda + \frac{\varphi S_V I_P}{N_V} - (\delta+\nu)I_V \qquad (6)$$

As a result, the nonlinear model for the transmission dynamics of the phyllody disease in sesame is summarized using parameters in Table 1 and the rates of change in the system (7).

$$\begin{aligned}
\frac{dS_P}{dt} &= rS_P\left(1-\frac{S_P+E_p+I_P}{K}\right) - \frac{(1-\psi)\alpha S_P I_V}{N_P} - \mu_P S_p \\
\frac{dE_p}{dt} &= \frac{(1-\psi)\alpha S_P I_V}{N_P} - (\kappa+\mu_P)E_P \qquad (7)\\
\frac{dI_P}{dt} &= \kappa E_p - (\rho+\tau+\mu_P)I_P \\
\frac{dS_V}{dt} &= \omega\Lambda - \frac{\varphi S_V I_P}{N_V} - (\delta+\nu)S_V \\
\frac{dI_V}{dt} &= (1-\omega)\Lambda + \frac{\varphi S_V I_P}{N_V} - (\delta+\nu)I_V
\end{aligned}$$

with initial conditions; $S_P(0) > 0; E_p \geq 0,\ I_P(0) \geq 0; S_V(0) \geq 0; I_V(0) \geq 0.$

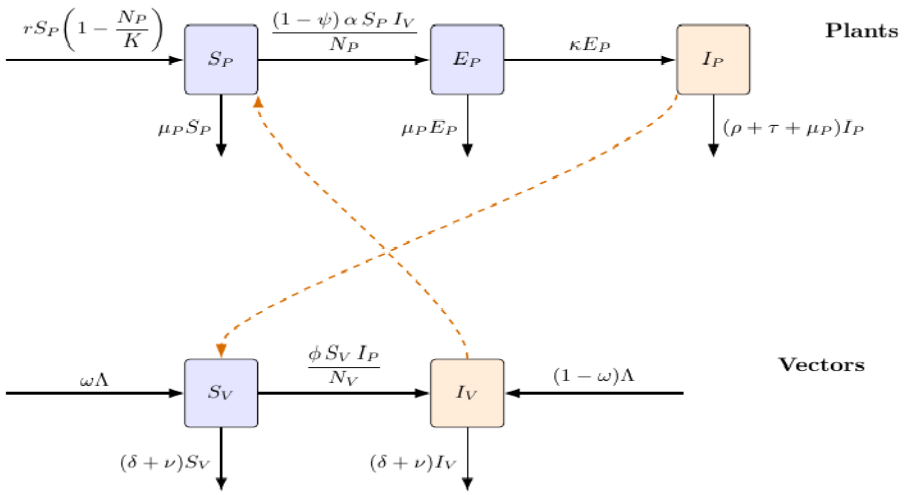

Figure 1: Transmission dynamics of Phyllody disease: solid lines represent the rates of transfer in and out of compartments, while dotted lines indicate interactions between sesame plants and vectors in the farm.

Table 1: Parameters and variables of Phyllody disease model (7).

Parameter	Description	Values	Source
r	Intrinsic growth rate of sesame plants	$0.5\ day^{-1}$	(Yemata and Bekele (2024)
K	Carrying capacity of the farm	$10000\ day^{-1}$	(Texas and AgriLife 2007)
α	Transfer rate of phytoplasma from I_V to S_p	$0.1 - 0.45\ day^{-1}$	(Alemneh et al. 2019)
ρ	Disease induced death rate on plant	$0.55\ day^{-1}$	(Reddy et al. 2019)
δ	Natural death rate of the leafhoppers	$0.03 - 0.04\ day^{-1}$	(Weintraub 2006)
ϕ	The rate at which vectors acquire infection by feeding on infected plants	$0.01 - 0.2\ day^{-1}$	(Vemana eta al 2023)
Λ	Recruitment rate of vectors into the farm	$0.005\ day^{-1}$	Assumed
ω	Probability of vectors entering the farm	$0 - 1\ day^{-1}$	Assumed
Ψ	Biological controls done before planting	$0 - 1\ day^{-1}$	(Alemneh et al. 2019)
τ	Roguing rate of the infected plants	$0 - 1\ day^{-1}$	Assumed
ν	Death rate of leafhoppers due to chemicals	$0 - 1\ day^{-1}$	(Alemneh et al. 2019)
μ_P	Sesame natural death rate	$0.003\ day^{-1}$	(Texas and AgriLife, 2007)
κ	Progression rate from exposed to infectious plants	$0.024\text{-}0.071\ day^{-1}$	(Gogoi et al.2017)

Variable	Description	Values	Source
S_p	Susceptible sesame plants	6000	Assumed
E_P	Exposed Sesame plants (Infected no sign)	200	Assumed
I_p	Infected and infectious sesame plants	200	Assumed
S_v	Susceptible Vectors (Leaf-hoppers)	120	Assumed
I_v	Infected and Infectious vectors (Leaf-hoppers)	600	Assumed

Qualitative behavior of the model

Here, properties of the model system (7) including the invariant region, positivity of the solution, existence of the equilibrium points and uniqueness of solutions are studied.

The Invariant region

The solution set of the Phyllody disease model in the system (7) are feasible for all t > 0 if all inters the invariant region $\mathfrak{B} = \{(S_P, E_p, I_P, S_V, I_V) \in \mathbb{R}^5_+ : \mathfrak{B}_p, \mathfrak{B}_v\}$.

Theorem 3.1. *(Positive invariance)*

Define

$$\bar{\sigma} = max\{N_{P(0)}, K\},$$
$$v = min\{\mu_P, (\rho + \tau)\}.$$

Then the region given by

$$\mathfrak{B} = \left\{(S_P, E_p, I_P, S_V, I_V) \in \mathbb{R}^5_+ : N_P(t) \leq \frac{r\bar{\sigma}}{v}; N_V(t) \leq \frac{\Lambda}{\delta + \nu}\right\}$$

is positively invariant with respect to the model system (7).

Proof. For the plants population in the system (7), $N_P = S_P + E_p + I_P$. That is

$$\frac{dN_P}{dt} = rS_P\left(1 - \frac{N_P}{K}\right) - \mu_P(S_P + E_P) - (\rho + \tau)I_P \leq rS_P - \mu_P(S_P + E_P) - (\rho + \tau)I_P$$

Since $v \leq \mu_P$ and $v \leq (\rho + \tau)$,
we have $\mu_P(S_P + E_P) + (\rho + \tau)I_P \geq v(S_P + E_P + I_P) = vN_P$.

Hence, $\frac{dN_P}{dt} \leq rS_P - vN_P \leq r\bar{\sigma} - vN_P$.
Therefore,
$$\frac{dN_P}{dt} + vN_P \leq r\bar{\sigma} \quad (8)$$

Solving the linear differential inequality (8) by the integrating-factor method gives
$N_{P(t)} \leq \left(\frac{r\bar{\sigma}}{v}\right)(1 - e^{-vt}) + N_P(0)e^{-vt}$,
So, that $\limsup_{t\to\infty} (N_{P(t)}) \leq \frac{r\bar{\sigma}}{v}$.
Thus, the plant component is confined to $\mathfrak{B}_p = \left\{ (S_P, E_P, I_P) \in R_+^3 : N_P \leq \frac{r\bar{\sigma}}{v} \right\}$.
Similarly, for the population of vectors, $N_V = S_V + I_V$. Taking the derivative of N_V then,
$$\frac{dN_V}{dt} = \Lambda - (\delta + \nu)N_V \quad (9)$$
Solving by the separation of variables technique, equation (10) becomes
$$N_V = \frac{\Lambda}{\delta+\nu} + \left(N_V(0) - \frac{\Lambda}{\delta+\nu}\right)e^{-(\delta+\nu)t} \quad (10)$$
Then, $\lim_{t\to\infty} N_V(t) \leq \frac{\Lambda}{\delta+\nu}$. Therefore,
$$\mathfrak{B}_V = \left\{(S_V, I_V) \in \mathbb{R}_+^2 : N_V \leq \frac{\Lambda}{\delta+\nu}\right\} \quad (11)$$
Combining $\mathfrak{B}_p$ and $\mathfrak{B}_V$ yields the positively invariant region $\mathfrak{B}$ stated in the theorem,
which completes the proof.

Positivity of the solutions

For the model system (7) to be biologically meaningful, it is important to prove that all of its solutions remain positive for all $t > 0$ and hence the following theorem:
Theorem 3.2. *If*
$\mathfrak{B} = \left\{\left(S_P, E_p, I_P, S_V, I_V\right) \in \mathbb{R}_+^5 : S_P > 0, E_p > 0, I_P > 0, S_V > 0, I_V > 0\right\}$, *then, the solution set* $\left\{S_P, E_p, I_P, S_V, I_V\right\}$ *of the model system is positive for all* $t > 0$.
Proof. We first show that whenever a component reaches zero, its time derivative is nonnegative, so trajectories cannot cross into the negative orthant.
(i) If $S_P = 0$, then
$$\frac{dS_P}{dt} = r \times 0\left(1 - \frac{N_P}{K}\right) - \frac{(1 - \psi)\alpha \times 0 \times \mathrm{I_V}}{\mathrm{N_P}} - \mu_\mathrm{P} \times 0 = 0 \geq 0.$$
(ii) If $E_P = 0$, then
$$\frac{dE_P}{dt} = \frac{(1 - \psi)\alpha S_P \mathrm{I_V}}{\mathrm{N_P}} - \kappa \times 0 - \mu_P \times 0 \geq 0.$$
(iii) If $I_P = 0$, then
$$\frac{dI_P}{dt} = \kappa E_P - (\rho + \tau) \times 0 = \kappa E_P \geq 0.$$
(iv) If $S_V = 0$ (so $N_V = I_V$), then
$$\frac{dS_V}{dt} = \omega\Lambda - \varphi \times 0 \times \frac{I_P}{N_V} - (\delta + \nu) \times 0 = \omega\Lambda \geq 0.$$
(v) If $I_V = 0$ (so $N_V = S_V$), then
$$\frac{dI_V}{dt} = (1 - \omega)\Lambda + \varphi S_V \frac{I_P}{N_V} - (\delta + \nu) \times 0 \geq 0.$$
Thus, each coordinate hyperplane is repelling (or neutral), and the nonnegative orthant is forward invariant
In addition, we do comparison for the inequalities and explicit lower bounds
Using $\frac{(1-\psi)\alpha S_P \mathrm{I_V}}{\mathrm{N_P}} \geq 0$ and $\varphi \mathrm{S_V} * \frac{\mathrm{I_P}}{\mathrm{N_V}} \geq 0$, we obtain $\frac{dS_P}{dt} \geq -\mu_P * S_P$,
$\frac{dE_P}{dt} \geq -(\kappa + \mu_P) * E_P$, $\frac{dI_P}{dt} \geq -(\rho + \tau) * I_P$ and $\frac{dS_V}{dt} \geq -(\delta + \nu)\mathrm{S_V} + \omega\Lambda$.
Solving these scalar linear inequalities gives
$S_{P(t)} \geq \mathrm{S_{P(0)}} e^{-\mu_P t} \geq 0$, As $t \to \infty, S(\mathrm{t}) \leq K$. Hence, $0 \leq S_{p(t)} \leq K$. Similarly,
$E_{P(t)} \geq E_{P(0)}e^{(-(\kappa + \mu_P)*t)} \geq 0$, $I_{P(t)} \geq I_{P(0)}e^{-(\rho+\tau)*t} \geq 0$,
$I_{V(t)} \geq I_{V(0)}e^{-(\delta+\nu)*t} \geq 0$ and $S_{V(t)} \geq \left[\frac{\omega\Lambda}{\delta+\nu}\right]\left(1 - e^{-(\delta+\nu)*t}\right) + S_{V(0)}e^{-(\delta+\nu)*t} \geq 0$
Combining Steps 1 and 2 completes the positivity proof. This assures that all variables of the model system (7) are all positivity. □

Phyllody- Disease free equilibrium point, $\mathfrak{D}_0$

The Phyllody disease free equilibrium point (assume no vertical transmission to vectors, i.e., $(1-\omega)\Lambda = 0$) is found when $I_P = E_p = I_V = 0$. Hence, the Phyllody disease free equilibrium point of the model system (7) is

$\mathfrak{D}_0 = \left(\mathrm{K} * \left(1 - \frac{\mu_P}{r}\right), 0, 0, \frac{\Lambda}{\delta + \nu}, 0\right)$.

Effective reproduction number

The effective reproduction number (R_e) is an average number of infections caused by a case of an infectious disease in a population introduced in a purely susceptible population (Khan et al. 2018, Mbuthia and Chepkwony 2019, Chuma and Mwanga 2020). In this work, R_e is determined using the Next Generation matrix method as used in (van den Driessche and Watmough 2002, Collins and Duffy 2022, Naaly et al. 2024, Olaniyi et al. 2025).

The system of equations governing the spread of infection is given by

$$\frac{dE_P}{dt} = \frac{(1-\psi)\alpha S_P I_V}{N_P} - (\kappa + \mu_P)E_P$$
$$\frac{dI_P}{dt} = \kappa E_P - (\rho + \tau)I_P$$
$$\frac{dI_V}{dt} = \frac{\varphi S_{VI_P}}{N_V} - (\delta + \nu) * I_V$$

The new infection terms, denoted by $\mathcal{F}$, and transition terms denoted by $\mathcal{V}$ are:

$\mathcal{F} = \begin{pmatrix} \frac{(1-\psi)\alpha S_P I_V}{N_P} \\ 0 \\ \frac{\varphi S_V I_P}{N_V} \end{pmatrix}$ and $\mathcal{V} = \begin{pmatrix} (\kappa + \mu_P)E_P \\ (\rho + \tau)I_P - \kappa E_P \\ (\delta + \nu)I_V \end{pmatrix}$, respectively. The Jacobian matrices evaluated at the disease-free equilibrium point, $\frac{S_P^*}{N_P^*} = 1$ and $\frac{S_V^*}{N_V^*} = 1$, so the Jacobians of F and V (with state order (E_p, I_p, I_v) are $F = \begin{pmatrix} 0 & 0 & \frac{(1-\psi)\alpha S_P^*}{N_P} \\ 0 & 0 & 0 \\ 0 & \frac{\varphi S_V^*}{N_V^*} & 0 \end{pmatrix} = \begin{pmatrix} 0 & 0 & (1-\psi)\alpha \\ 0 & 0 & 0 \\ 0 & \varphi & 0 \end{pmatrix}$, and

$$V = \begin{pmatrix} \kappa + \mu_P & 0 & 0 \\ -\kappa & \rho + \tau & 0 \\ 0 & 0 & \delta + \nu \end{pmatrix}$$

Using the next generation matrix method, the effective reproduction number, R_e, of the system (7) is given as the dominant eigenvalue of matrix FV^{-1} (Goswami et al. 2024, Olaniyi et al. 2025).

The nonzero infection cycle is $E_P \rightarrow I_V$ via I_P progression, giving eigenvalues $\pm\sqrt{ab}$, where:

$a = \frac{(1-\psi)\alpha}{(\delta + \nu)}$, and $b = \frac{\varphi \kappa}{[(\kappa + \mu_P)(\rho + \tau)]}$

Thus, the effective reproduction number; $R_e = \sqrt{\frac{(1-\psi)\alpha\varphi\kappa}{(\kappa + \mu_P)(\rho + \tau)(\delta + \nu)}}$ (19)

Evaluating equation (19) in the absence of control measures such that when $\psi = \tau = \nu = 0$, the effective reproduction number, R_e, reduced to basic reproduction number as shown in equation

$R_0 = \sqrt{\frac{\alpha\varphi\kappa}{(\kappa + \mu_P)\rho\delta}}$ (20)

Local stability of the Phyllody- disease-free equilibrium point of the model

Theorem 3.3. *The disease-free equilibrium point, $\mathfrak{D}_0$, is locally asymptotically stable if $R_0 < 1$ and unstable whenever $R_0 > 1$.*

Proof. The Jacobian matrix of the model system (7) evaluated at, $\mathfrak{D}_0$ is:

$$J_{\mathfrak{D}_0} = \begin{pmatrix} -(r - \mu_P) & -\frac{r}{K}S_P^0 & -\frac{r}{K}S_P^0 & 0 & -(1-\psi)\alpha \\ 0 & -(\kappa + \mu_P) & 0 & 0 & (1-\psi)\alpha \\ 0 & \kappa & -(\rho + \tau + \mu_P) & 0 & 0 \\ 0 & 0 & -\varphi & -(\delta + \nu) & 0 \\ 0 & \varphi & \varphi & 0 & -(\delta + \nu) \end{pmatrix}$$

From the Jacobian evaluated at the disease-free equilibrium , $\mathfrak{D}_0$, one eigenvalue comes from the plant logistic direction, $\lambda_1 = -(r - \mu_P)$, and another from the vector demographic mode, $\lambda_2 = -(\delta + \nu)$. The remaining three eigenvalues are obtained as the roots of the characteristic equation of the infected/latent subsystem using the following characteristic polynomial equation:

From the variational matrix, two of the eigenvalues are $\lambda_1 = -r$ and $\lambda_2 = -(\delta + \nu)$. The remaining eigenvalues are found using the following polynomial characteristic equation,

$\lambda^3 + (a + b + c)\lambda^2 + (ab + ac + bc)\lambda + (abc - \beta\kappa\varphi) = 0$ (21)

with $a = \kappa + \mu_{P>0}$, $b = \rho + \tau + \mu_P > 0$, $c = \delta + \nu > 0$, and $\beta = (1 - \psi)\alpha > 0$ if $\psi < 1$. Thus, $a_2 = (a + b + c) > 0$ and $a_1 = (ab + ac + bc) > 0$ always.

Let $a_0 := a\,b\,c - \beta\,\kappa\,\varphi$ (the constant term of the characteristic polynomial (22)

Then, $a_0 = abc - \beta\kappa\varphi = abc(1 - R_0^2)$. Thus, the sign of a_0 depends only on R_0.

Specifically, if $a_0 > 0 \Leftrightarrow R_0 < 1$, or $a_0 = 0 \Leftrightarrow R_0 = 1$ or $a_0 < 0 \Leftrightarrow R_0 > 1$.

Table 2: Descartes' Rule of Sign conditions for at most two positive real roots determined based on R_0 for the Sesame model

Case	a_2	a_1	$a_0 = a\,b\,c\,(1 - R_0^2)$	R_0	Sign changes	Number of Positive real roots	Interpretation
A	+	+	+	$R_0 < 1$	0	0	$\mathfrak{D}_0$ locally asymptotically stable
B	+	+	0	$R_0 = 1$	-	-	Threshold (Transcritical point)
C	+	+	-	$R_0 > 1$	1	1	One positive eigenvalue; invasion

In our Sesame model, only two sign patterns occur: $a_2 > 0, a_1 > 0$ with $a_0 > 0$, (Case A) when $R_0 < 1$, and $a_2 > 0, a_1 > 0$ with $a_0 < 0$, (Case C) when $R_0 > 1$; the threshold $a_0 = 0$ corresponds to $R_0 = 1$ (Case B). Thus, for $R_0 < 1$ the disease-free equilibrium $\mathfrak{D}_0$ is locally asymptotically stable; for $R_0 > 1$ there is exactly one sign change, yielding one positive real root and loss of stability (invasion). Because a_2 and a_1 are always positive in this model, the mixed-sign cases that would permit backward bifurcation do not arise; accordingly, Descartes' Rule of Signs implies at most one positive real root.

Global stability of disease-free equilibrium point

Global stability of the model system is established to determine if the disease can persist or removed from the sesame population. Mathematical proof is presented using a Lemma described in (Castillo-Chavez et al 2002, Chuma and Mwanga 2019, Collins and Duffy 2022, Goswami et al. 2024).

Lemma 3.1. *Consider a model system written in the form*

$$\frac{db}{dt} = B(b, g)$$
$$\frac{dg}{dt} = G(b, g), G(b^*, 0) = 0$$

where $b \in R^m$ *and* $g \in R^n$. *The disease-free equilibrium point of the model system (7) is denoted by* $(b_1^*, 0)$ *assuming that*

(i) $\frac{db}{dt} = B(b, 0)$, b^* *is globally asymptotically stable,*

(ii) $G(b, g) = TI - \hat{G}(b, g), \hat{G}(b, g) \geq 0, \ \forall (b, g) \in \mathfrak{B}$

where $\mathfrak{B}$ *is the invariant region of the model system (7) and* $T = \frac{\partial G(b,0)}{\partial g}$ *is an* $M -$ *matrix with non-negative off diagonal elements.*

Theorem 3.4. *The disease-free equilibrium point of the model system* (7) *is globally asymptotically stable if* $R_e < 1$.

Proof. Using Lemma (3.1), we need to show that conditions (i) and (ii) holds for $R_e < 1$. From the model system (7), the susceptible population are given by $b = (S_P, S_V) \in \mathbb{R}^2$ and the infectious populations are given by $g = (E_P, I_P, I_V) \in \mathbb{R}^2$. Then, when $g = 0$ we have,

$$\frac{db}{dt} = B(b, 0) = \begin{pmatrix} rS_P\left(1 - \frac{S_P}{K}\right) - \mu_P S_P \\ \omega\Lambda - (\delta + \nu)S_V \end{pmatrix} \quad (23)$$

using the separation of variables technique, the solutions of the system (23) are therefore

$$S_P(t) = \frac{K(1 - \frac{\mu_P}{r})}{1 + Ce^{-(r - \mu_P)t}}, \text{ where } C = \frac{K\left(1 - \frac{\mu_P}{r}\right) - S(0)}{S(0) - 1} \text{ and } S_V(t) = \frac{\omega\Lambda}{(\delta + \nu)} + \left[S_{V(0)} - \frac{\omega\Lambda}{(\delta + \nu)}\right] e^{-(\delta + \nu)t}.$$

As $t \to \infty$, we have $S_{P(t)} \to K\left(1 - \frac{\mu_P}{r}\right)$ and $S_{V(t)} \to \frac{\omega\Lambda}{(\delta + \nu)}$.

Therefore, b^* is globally asymptotically stable, confirming that condition (i) holds. Looking back for condition (ii), we have;

$$\frac{dg}{dt} = G(I_P, I_V) = \begin{pmatrix} \frac{(1-\psi)\alpha S_P I_V}{N_P} - (\kappa + \mu_p)E_p \\ \kappa E_p - (\rho + \tau + \mu_P)I_p \\ (1-\omega)\Lambda + \frac{\varphi S_V I_P}{N_V} - (\delta + \nu)I_V \end{pmatrix} \quad (24)$$

Then, the Jacobian matrix of (24) evaluated at $\mathfrak{D}_0$ is

$$T = \begin{pmatrix} -(\kappa + \mu_P) & 0 & (1-\psi)\alpha \\ \kappa & -(\rho + \tau + \mu_P) & 0 \\ 0 & \varphi & -(\delta + \nu) \end{pmatrix} \quad (25)$$

Using Equations (24) and (25), and define $\widehat{G}(b,g)$ component wise we obtain

$$\begin{pmatrix} \widehat{G_1}(b,g) \\ \widehat{G_2}(b,g) \\ \widehat{G_3}(b,g) \end{pmatrix} = \begin{pmatrix} \left((1-\psi)\alpha \left[1 - \frac{S_P}{N_P}\right] I_V\right) \\ 0 \\ \varphi \left[1 - \frac{S_V}{N_V}\right] I_P \end{pmatrix} \quad (26)$$

From the system in (26), each component of $\widehat{G_i}(b,g), (i = 1,2,3)$, is nonnegative on the feasible region Ω (because $0 \leq \frac{S_P}{N_P} \leq 1$ and $0 \leq \frac{S_V}{N_V} \leq 1$. Hence, condition (ii) holds. Consequently, when $R_e \leq 1$, the disease-free equilibrium point is globally asymptotically stable and hence the theorem (3.6) holds.

Bifurcation analysis

We use the Centre manifold theorem stated in (Castillo-Chavez and Song 2004, Mushayabasa et al. 2017, Chuma and Mwanga. 2020, Olaniyi et al. 2023) to investigate the changes on R_0 close to a unit.

Theorem 3.5. *Consider the following general system of ordinary differential equations with a bifurcation parameter* α,

$$\frac{dx}{dt} = f(x,\alpha), g: \mathbb{R}^n \times \mathbb{R} \; and \; f \in C^n(\mathbb{R}^n \times \mathbb{R}) \quad (27)$$

Without loss of generality, it is assumed that 0 *is an equilibrium for system (27) for all values of the parameter* α*; that is,* $f(0,\alpha) = 0$ *for all* $\alpha > 0$*. Now, assume that;*

(i) $E = D_x f(0,0) = \frac{\partial f_i}{\partial dx_j}(0,0)$ *is the linearization of system (27) around the equilibrium* 0

with f *evaluated at* 0*. Zero is a simple eigenvalue of* E*, and other eigenvalues of* E *have negative real parts.*

(ii) *Matrix* E *has a right eigenvector* w *and a left eigenvector* v *corresponding to the zero eigenvalue. Let* f_k *be the* k^{th} *component of* f *and*

$$a = \sum_{k,i,j=1}^{n} v_k w_i w_j \frac{\partial^2 f_k}{\partial x_i \partial x_j}(0,0)$$

$$b = \sum_{i,k=1}^{n} v_k w_i \frac{\partial^2 f_k}{\partial x_i \partial \alpha}(0,0) \quad (28)$$

The local dynamics of the system (27) around $(0,0)$ *are governed by the signs of* a *and* b *in the following conditions:*

(i) $a > 0, b > 0$*. When* $q < 0$ *with* $|\alpha| \ll 1$, $(0,0)$ *is locally asymptotically stable, and there exists a positive unstable equilibrium; when* $0 < \alpha \ll 1$*, 0 is unstable and there exists a negative and locally asymptotically stable equilibrium.*

(ii) $a < 0, b < 0$*, when* $\alpha < 0$ *with* $|\alpha| \ll 1$, $(0,0)$ *is unstable; when* $0 < \alpha \ll 1$, 0 *is locally asymptotically stable, and there exists a positive unstable equilibrium.*

(iii) $a > 0, b < 0$, *when* $\alpha < 0$ *with* $|\alpha| \ll 1$, $(0,0)$ *is unstable; and there exists a locally asymptotically stable negative equilibrium; when* $0 < \alpha \ll 1$, $(0,0)$ *is stable, and a positive unstable equilibrium appears.*

Theorem 3.6. *The endemic equilibrium point of the model became locally asymptotically stable whenever* $R_0 > 1$.

Proof. On introducing new variables to the model sub-systems (7), such that $S_P = x_1$, $E_P = x_2$, $I_P = x_3$, $S_V = x_4$, $I_V = x_5$, and normalize the total plant and vector populations so that $N_P = n_P = 1$ and $N_V = n_V = 1$ that then model system can be re-written as follows;

$$\begin{aligned} \frac{dx_1}{dt} &= rx_1\left(1 - \frac{x_1 + x_2 + x_3}{K}\right) - (1-\psi)\alpha x_1 x_5 - \mu_P x_1 \\ \frac{dx_2}{dt} &= (1-\psi)\alpha x_1 x_5 - (\kappa + \mu_P) * x_2 \\ \frac{dx_3}{dt} &= \kappa x_2 - (\rho + \tau + \mu_P)x_3 \\ \frac{dx_4}{dt} &= \omega\Lambda - \varphi x_4 x_3 - (\delta + \nu)x_4 \\ \frac{dx_5}{dt} &= (1-\omega)\Lambda + \varphi x_4 x_3 - (\delta + \nu)x_5 \end{aligned} \quad (29)$$

Using equation (19), take alpha (α) as the bifurcation parameter. Setting $R_e(\alpha) = 1$ gives:

$\alpha^\star = \frac{((\kappa+\mu_P)(\rho+\tau)(\delta+\nu))}{((1-\psi)\phi\kappa)}$ and the disease-free equilibrium point of the model system (29) is

$\mathfrak{D}_0 = \left(S_P^0, E_P^0, I_P^0, S_V^0, I_V^0 \right) = \left(K\left(1 - \frac{\mu_P}{r}\right), 0, 0, \omega\frac{\Lambda}{\delta+\nu}, (1-\omega)\frac{\Lambda}{\delta+\nu} \right)$. The linearizes matrix of the model system (29) about the disease-free equilibrium pointx_0 at
$\alpha = \alpha_0^*$ becomes

$$J_{\mathfrak{D}_0}(\alpha^*) = \begin{pmatrix} a_{11} & -(r-\mu_p) & -(r-\mu_p) & 0 & -(1-\psi)\alpha^* S_p^0 \\ -(1-\psi)\alpha^* I_V^0 & -(\kappa+\mu_p) & 0 & 0 & -(1-\psi)\alpha^* S_p^0 \\ 0 & \kappa & -(\rho+\tau+\mu_p) & 0 & 0 \\ 0 & 0 & -\varphi S_V^0 & -(\rho+\nu) & 0 \\ 0 & 0 & \varphi S_V^0 & 0 & -(\rho+\nu) \end{pmatrix}$$

where $a_{11} = r\left(1 - \frac{2S_p^0}{K}\right) - \mu_p - (1-\psi)\,\alpha^* I_V^0$.
Let $J_{\mathfrak{D}_0}(\alpha^*)$ be the Jacobian of system (29) at $\mathfrak{D}_0$ and threshold α^*.
The right eigenvector $(w = (w_1, w_2, w_3, w_4, w_5)^T$ of system (29) associated with the simple zero eigenvalues, (i.e. $J_{\mathfrak{D}_0}(\alpha^*)w = 0$) can be parameterized by ($w_2 \neq 0$ as

$W_3 = \left(\frac{\kappa}{\rho+\tau+\mu_P}\right) w_2$, $w_4 = -\left(\varphi\frac{S_{V0}}{\delta+\nu}\right) w_3$, $w_5 = \left(\varphi * \frac{S_{V0}}{\delta+\nu}\right) * w_3, w_1 = \frac{(\kappa+\mu_p)w_2 - (1-\varphi)\alpha^* S_p^0 w_5}{(1-\psi)\alpha^* I_V^0}$

with $S_{P0} = K\left(1 - \frac{\mu_P}{r}\right), S_{V0} = \omega\frac{\Lambda}{\delta+\nu}, I_{V0} = (1-\omega)\frac{\Lambda}{\delta+\nu}$.
In addition, the left eigenvector $v = (v_1, v_2, v_3, v_4)^T$ of system (29) associated with zero eigenvalues, is given as follows:
First choose $v_2 \neq 0$ and set$V_1 = -\left(\frac{(1-\psi)\alpha^* I_V^0}{a_{11}}\right) v_2$,

$v_3 = \frac{(r-\mu_P)v_1 + (\kappa+\mu_p)v_2}{\kappa}$, $v_4 = 0$, and $v_5 = \left(\frac{(1-\psi)\alpha^* S_P^0}{\delta+\nu}\right)(v_2 - v_1)$

Using the center–manifold formulas, Eq. (28), the bifurcation coefficients at the DFE (with $\alpha = \alpha^*$), first we have $b = (1-\psi)\,[\,(v_2 - v_1)\,(I_V^0 w_1 + S_P^0 w_5)]$
Using the eigenvector identity (substitute w_1 and w_5), $I_V^0 w_1 + S_P^0 w_5 = \frac{\kappa+\mu_P}{(1-\psi)\alpha^*} w_2$, we obtain the closed form $b = (\kappa+\mu_P)(v_2 - v_1)w_2$. All factors are positive for the chosen scaling $i.e\ \ \kappa + \mu_P > 0,\ \alpha^* > 0, v_2 - v_1 > 0$, and $w_2 > 0$. Hence, $b > 0$. Also, we have

$$a = v_1\left[-\frac{r}{K}w_1^2 - \frac{r}{K}w_1 w_2 - \frac{r}{K}w_1 w_3 - (1-\psi)\alpha^* w_1 w_5\right] + v_2[\,(1-\psi)\alpha^* w_1 w_5] + v_{4[-\varphi\, w_3 w_4]} + v_5[+\varphi\, w_3 w_5$$

with the eigenvector relations above one has $w_2 > 0, w_3 > 0, w_5 > 0$, and typically $w_1 \leq 0$ at α^*.
Hence the logistic curvature contributes a strictly negative term $-\frac{r}{K}v_1 w_1^2 < 0$, the mixed logistic terms $-\frac{r}{K}v_1 w_1(w_2 + w_3) \leq 0$, and $(v_2 - v_1)(1-\psi)\alpha^* w_1 w_5 \leq 0$ because $(v_2 - v_1) > 0$, $w_5 > 0$, $w_1 \leq 0$. The only positive contribution is $v_5 \varphi w_3 w_5 > 0$.
In the present model (with $r > 0, K > 0, \varphi > 0$, and $w_1 \leq 0$ under the threshold α^*, the negative curvature terms dominate, yielding $a < 0$.
Therefore, since the coefficients $b > 0$ and $a < 0$ using Theorem (3.5), it is sufficed to conclude that the model system (7) undergoes a forward bifurcation at $R_e = 1$. These results assure us that the phyllody disease can be eradicated from the sesame field if proper control measures are well maintained.

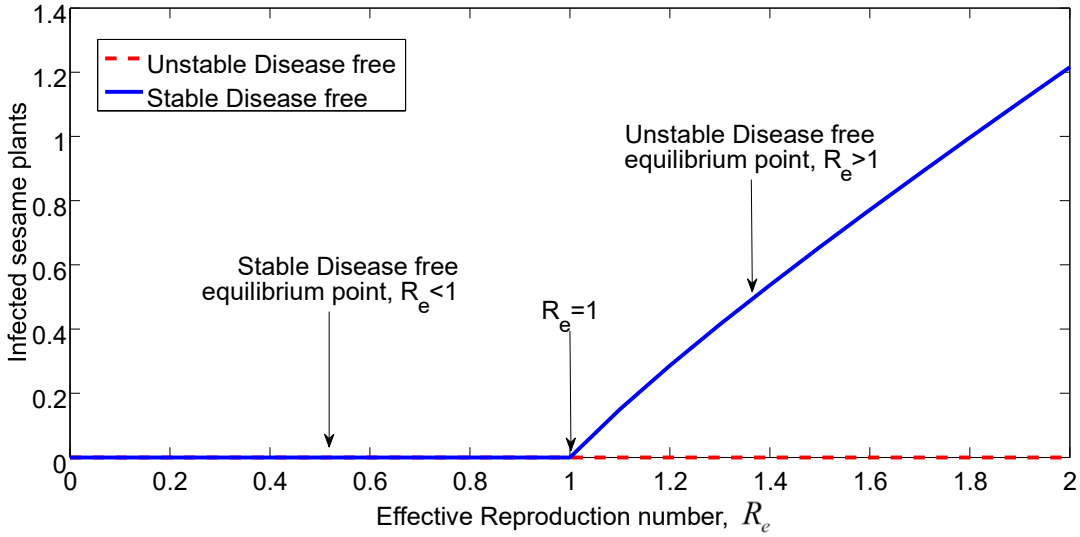

Figure 2: Bifurcation analysis of the Equilibrium points of the sesame model 7.

The parameters of the model chosen for $R_e = 0.0328; \delta = 0.04; \rho = 0.00055;\ \varphi = 0.01667; K = 10000;$ $\alpha = 0.45; \psi = 0.69; \tau = 0.8;\ \nu = 0.512, \kappa = 0.0475$ and $\mu_P = 0.0033$

Endemic equilibrium point

In the persistence of the disease in the field, a model system 7 has the endemic equilibrium point

$$\mathfrak{D}_1 = \left(S_P^*, E_p, I_P^*, S_V^*, I_V\right)$$

Define $c_0 = \frac{(\rho + \tau + \mu_P)}{\kappa}$, and $c_1 = (\rho + \tau + \mu_P) * (\kappa + \mu_P) * \frac{N_P}{\kappa * (1-\psi) * \alpha}$.

Vector block:

$$S_V^* = \frac{\omega * \Lambda}{(\delta+\nu)\frac{\varphi}{N_V} I_P *}, I_V^* = \frac{(1-\omega)*\Lambda}{\delta+\nu} + \left(\omega \frac{\Lambda}{\delta+\nu}\right)\left(\frac{\frac{\varphi I_P}{N_V}}{(\delta+\nu)+\left(\frac{\varphi I_P}{N_V}\right)}\right)$$

Plant infection/progression:

$$E_P = c_0 I_P, \quad S_P = c_1 \frac{I_P}{I_V}$$

Global stability of endemic equilibrium point

Theorem 3.7. *The endemic point of the model system* (7) *is asymptotically in the invariant region stable when* $R_0 > 1$.

Proof: Now consider the Lyapunov function as used in Chuma and Mwanga 2020, Chuma and Ngailo et al. 2024, Liana and Chuma 2023 and Olaniyi and Chuma 2023, with state variables x^* and Lyapunov constants $\zeta_i(1,2,3,4,5)$

$$L = \zeta_1\left(S_P - S_P^* \ln\frac{S_P^*}{S_P}\right) + \zeta_2\left(E_P - E_P^* \ln\frac{E_P^*}{E_P}\right) + \zeta_3\left(I_P - I_P^* \ln\frac{I_P^*}{I_P}\right) + \zeta_4\left(S_V - S_V^* \ln\frac{S_V^*}{S_V}\right) + \zeta_5\left(I_V - I_V^* \ln\frac{I_V^*}{I_V}\right) \quad (30)$$

By taking the first derivative of equation (30), we have

$$\frac{dL}{dt} = \zeta_1\left(1 - \frac{S_P^*}{S_P}\right)\frac{dS_P}{dt} + \zeta_2\left(1 - \frac{E_P^*}{E_P}\right)\frac{dE_P}{dt} + \zeta_{23}\left(1 - \frac{I_P^*}{I_P}\right)\frac{dI_P}{dt} + \zeta_4\left(1 - \frac{S_V^*}{S_V}\right)\frac{dS_V}{dt} + \zeta_5\left(1 - \frac{I_V^*}{I_V}\right)\frac{dI_P}{dt} \quad (31)$$

with the model system (7) at the endemic equilibrium point, pick weights to cancel incidence terms:

$$\zeta_S = \zeta_E, \text{and } \zeta_{SV}\, I_P = \zeta_{IV}\, S_V$$

with the above choices, all incidence cross-terms cancel and equation (31) simplifies to

$$\begin{aligned}\frac{dL}{dt} = &-\left[\zeta_S\left(\frac{r}{K}\right)S^*{}_P\left(\frac{S_P}{S_P^*} - 1\right)^2 + \zeta_E * (\kappa + \mu_P) E_P^*\left(\frac{E_P}{E_P^*} - 1\right)^2\right] \\ &- \left[\zeta_I(\rho + \tau + \mu_P) I_P^*\left(\frac{I_P}{I_P^*} - 1\right)^2 + \zeta_{S_V}(\delta+\nu) S_V^*\left(\frac{S_V}{S_V^*} - 1\right)^2\right] \\ &- \left[\zeta_{I_V}(\delta + \nu) I^*{}_V\left(\frac{I_V}{I_V^*} - 1^2\right)\right] \le 0.\end{aligned}$$

then $\frac{dL}{dt} \le 0$ iff $S_P = S_P^*, I_P = I_P^*, S_V = S_V^*$, and $I_V = I_V^*$. Hence, $\mathfrak{D}_1$ is the only set of the endemic equilibrium point in the invariant set $\mathfrak{B}$ for $R_e > 1$. Using the LaSalle invariant principle (LaSalle 1976), $\mathfrak{D}_1$ is globally asymptotically stable on the invariant set $\mathfrak{B}$.

Sensitivity analysis

Sensitivity analysis examines how uncertainty in model parameter inputs affects the model outputs. For Phyllody disease in sesame, sensitivity analysis is conducted to identify the model parameters that influence the effective reproduction number (R_e). A parameter is considered highly sensitive to R_e if its absolute value is greater than that of other parameters, regardless of its sign. Such highly sensitive parameters should be targeted for control measures to effectively reduce the number of new Phyllody infections in susceptible sesame plants.

The sensitivity analysis is performed using the Normalized Forward Sensitivity Index, which measures the proportional change in a variable relative to the proportional change in a parameter (Chitnis et al. 2008, Goswami et al. 2024). The Normalized Forward Sensitivity Index of the effective reproduction number (R_e) with respect to a parameter p is given by

$$\Upsilon_p^{R_e} = \frac{\partial R_e}{\partial p} \times \frac{p}{R_e},$$

where p represents any parameter influencing the effective reproduction number R_e. The model system (7) includes nine parameters: Namely, the biological controls done before planting, ψ, the per-contact transmission rate from infectious vectors to susceptible plants, α, the infection acquisition rate for vectors feeding on infectious plants, φ, the net plant recruitment/establishment rate feeding the susceptible plant pool, κ, the natural mortality rate of plants, μ_P, the disease-induced plant removal/mortality rate, ρ, the control-driven roguing/removal rate of infectious plants, τ, the natural mortality rate of vectors , δ, and the death rate of leafhoppers due to chemicals, ν. Additionally, setting the values for the model parameters such that $\alpha = 0.275, \rho = 0.55, \delta = 0.035, \kappa = 0.0475, \mu_P = 0.0033$, $\varphi = 0.105$, $\psi = 0.5, \tau = 0.5$, and $\nu = 0.5$. Thus, the normalized sensitivity index of R_e corresponding to the parameter α, which is the transfer rate of phylotoplasma from infected vectors to susceptible sesame plants is given as $\Upsilon_\alpha^{R_e} = \frac{\partial R_e}{\partial \alpha} \times \frac{\alpha}{R_e} = +0.5000$. Other indices are calculated using a similar approach and the results are displayed in Table 3.

Table 3: Sensitivity indices of the model parameters

Parameter	Sensitivity Index
ρ	-0.2619
ν	-0.4673
φ	$+0.5000$
τ	-0.2381
ψ	-0.5000
α	$+0.5000$
δ	-0.0327
κ	$+0.0297$
μ_P	-0.0297

For better clarity and visualization, the sensitivity indices from Table 3 are illustrated in Figure 3.

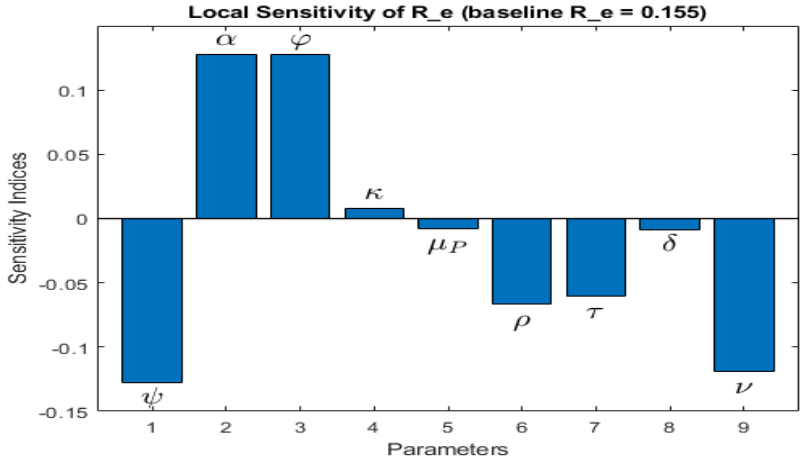

Figure 3: Sensitivity indices of R_e with respect to the model parameters.

The bar chart in Figure 3 shows the normalized local sensitivity indices of the effective reproduction number R_e with respect to the parameters ψ (pre-planting control intensity), α (vector-to-plant transmission rate), φ (plant-to-vector infection acquisition rate), κ (plant recruitment/establishment), μ_P (natural plant loss), ρ (disease-induced plant removal), τ (roguing/removal of infectious plants), δ (natural vector mortality), and ν (death rate of leafhoppers due to chemicals). It can be observed that the most sensitive parameters are α and φ (both positive) and, ψ and ν (both negative). Thus, increasing α or φ markedly raises R_e, making them key drivers of transmission, whereas increasing ψ or ν strongly reduces R_e, indicating powerful inhibitory effects. Parameters of moderate influence are τ and ρ, which have negative indices—raising either lowers R_e but with smaller impact than ψ or ν. The remaining parameters show weak effects: κ is slightly positive (a small increase raises R_e), while μ_P and δ are slightly negative (small increases reduce R_e). Therefore, to curb phyllody transmission most effectively, efforts should focus on decreasing α and φ, for example, reducing plant–vector contacts and vector acquisition, while increasing ψ and ν, for instance, strengthening pre-planting controls and vector mortality/emigration). Our results are consistent with prior studies: Gupta et al. (2022) reported that seed treatment and compatible insecticide programs (for example, imidacloprid with follow-up sprays) significantly lowered sesame phyllody incidence; Lukurugu et al. (2023) emphasized that high vector pressure and limited access to inputs in Tanzanian sesame systems make pre-season interventions especially important; and Yadav et al. (2023) found that integrated management treatments consistently reduced disease compared with unsprayed controls.

Results

This section presents different graphical solutions of the model system (7) by considering three control strategies: biological, roguing and the use of chemicals that are often applied purposely for controlling the phyllody disease of sesame plants. Numerical simulations were performed in MATLAB using the ODE45 solver with initial conditions: $S_P(0) = 6000$, $Ep(0) = 200$, $I_P(0) = 200$, $S_V(0) = 120$, $I_V(0) = 600$, and parameter values found in Table 1. The parameter values presented in Table 1 were selected based on published literature, agronomic recommendations, and biologically plausible assumptions necessitated by the limited availability of site-specific data on phyllody disease in sesame. All parameters were measured and expressed on a per-day basis, with population variables scaled at the farm level. Sesame is an annual crop with an average life span of approximately 90–120 days, which implies a natural plant mortality rate in the range $\mu_P \approx 0.01 - 0.03 \quad day^{-1}$ (Texas and AgriLife, 2007). The intrinsic growth rate of sesame plants was assumed to represent a moderate growth rate typical of short-cycle annual crops under favorable environmental conditions. This choice is consistent with

values commonly adopted in plant population and crop-disease models and was explored over the range $0.3 - 0.8\ day^{-1}$. In practice, this parameter is often inferred using Relative Growth Rate (RGR) measurements as a proxy (Yemata and Bekele 2024).
The carrying capacity, *K,* represents a realistic upper bound on farm-level sesame density based on standard planting densities and spacing practices. To assess model robustness, K was varied between 5,000 and 20,000 plants per hecter (Texas and AgriLife2007).

Phytoplasma transmission, including the transmission rate from infected vectors to susceptible plants is fiund to be in the range $0.1 \le \alpha \le 0.45\ day^{-1}$ as cited from Alemneh et al. (2019). Biological control effectiveness and the roguing rate of infected plants are ranging between $0 \le \psi, \tau \le 1$ adopted from Alemneh et al. 2019). Disease-induced mortality of plant was fixed at $\rho = 0.55\ day^{-1}$, following estimates reported by Reddy et al. (2019). The infection acquisition rate from infected plants ($\phi = 0.01 - 0.2\ day^{-1}$) was informed by Vemana et al. (2023). The adult life span of leafhoppers was assumed to the range from 14 to 45 days, yielding a natural vector mortality rate $\delta = 0.03 - 0.04\ day^{-1}$, consistent with entomological studies (Weintraub and Beanland 2007). The vector recruitment rate into the farm $\Lambda = 0.005\ day^{-1}$ was assumed within biologically reasonable ranges reported for similar agro-ecosystems. The progression rate from exposed to infectious plants, $\kappa = 0.024 - 0.071\ day^{-1}$, was adopted from Gogoi et al. (2017). The impact of each control strategy was examined separately, and the corresponding results are reported in the subsequent sections.

Effect of control strategies on the dynamics of phyllody disease

We now examine in detail the roles of biological control, chemical control, and roguing on the dynamics of Phyllody disease in sesame through simulation to evaluate the effectiveness of different management strategies.

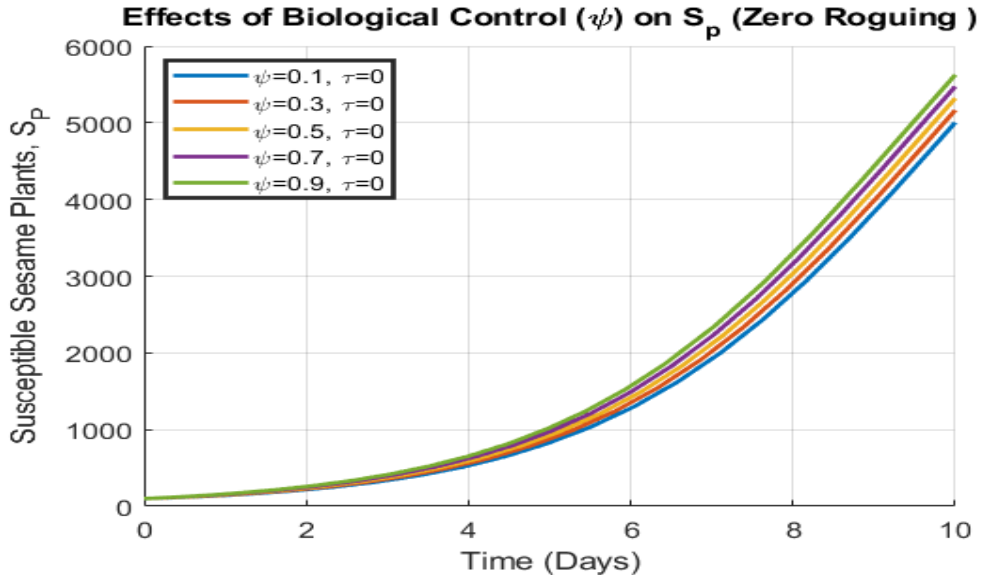

Figure 4: Effects of Biological controls taken on sesame seeds and the field before plantation.

Figure 4 shows (S_P) over the first 10 days after phyllody symptoms are observed, with varying biological control efficacy ψ and no roguing ($\tau = 0$). As ψ increases (0.1 to 0.9), reduced vector plant transmission lowers infection pressure, allowing more plants to remain uninfected and grow logistically, so S_P rises faster. Thus, higher ψ markedly preserves and boosts susceptible even without roguing.

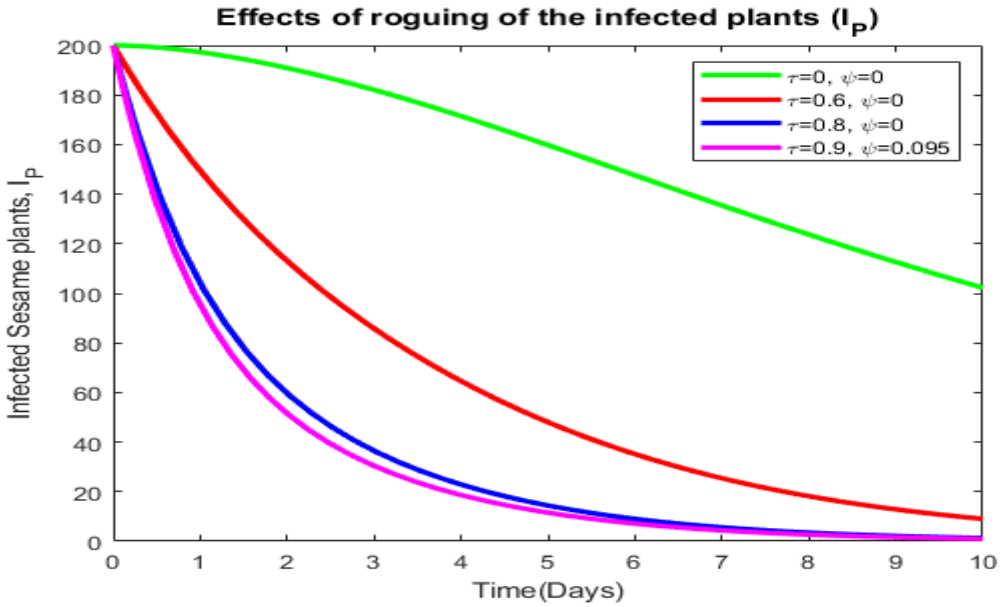

Figure 5: Effects of the roguing of the infected plants on the transmission rate of plasma from infected leafhoppers the sesame plants.

Figure 5 shows the number of infected sesame plants (I_P) decreases over the first 10 days after phyllody symptoms are observed, under different roguing rates ($\tau = 0,0.6,0.8,0.9$) and chemical control levels ($\psi = 0,095$). With no roguing of infected plants, infections decline slowly, while higher roguing rates accelerate the reduction of infections. The combination of a high roguing rate ($\tau = 0.9$) with high chemical control efficacy ($\psi = 0.095$) results in the steepest decline, demonstrating that integrated roguing and chemical control strategies are most effective in reducing Phyllody disease burden in sesame crops.

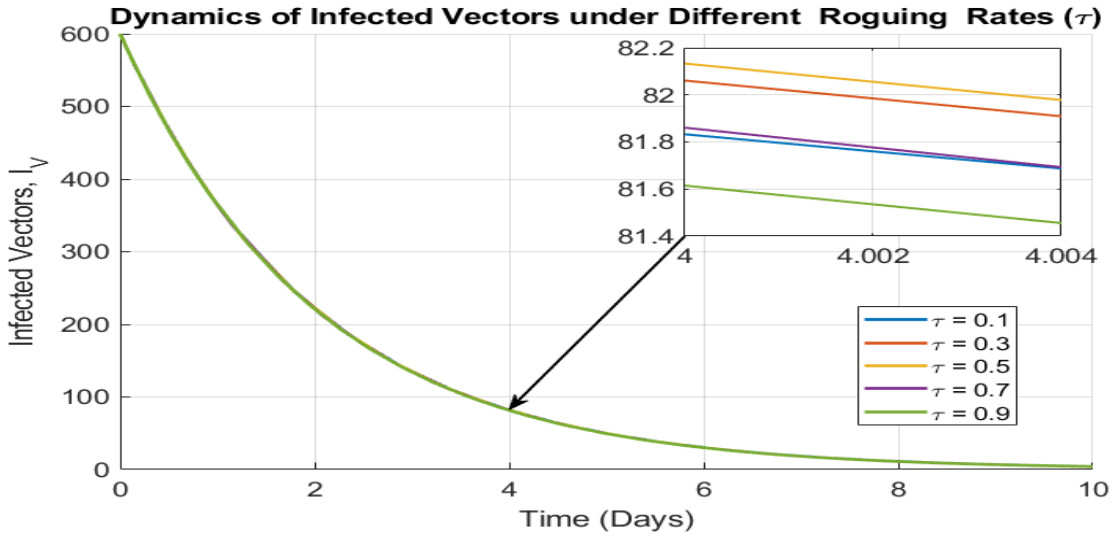

Figure 6: Effects of the roguing rates (τ) on the infected vector population.

Figure 6 shows the dynamics of infected vector I_V populations under different roguing rates (τ) over time for Sesame Phyllody management, during the first 10 days following the observation of phyllody symptoms. Across all τ values, the infected vector population declines gradually, demonstrating the effectiveness of control measures. Additionally, the inset zoom, captures a narrow window showing fine differences in the rates of decline under different τ values, where higher τ (e.g., 0.9) results in slightly slower declines in I_V than lower τ due to the absence of chemical control ($\psi = 0$), making the roguing affect vectors only indirectly by reducing infected hosts. The visible slope differences indicate that while higher τ reduces infected plants faster, its immediate effect on vectors is subtle. Using chemicals ($\psi > 0$) would directly reduce plant-to-vector transmission, steepening the decline in I_V across all τ values and emphasizing the benefit of combined strategies in Phyllody management. However, the decline in infected vector numbers is not tightly coupled to the roguing rate. For example, when $\tau = 0.1$ the infected-vector count is lower than at higher roguing rates ($\tau = 0.3, 0.4, 0.5, 0.7$

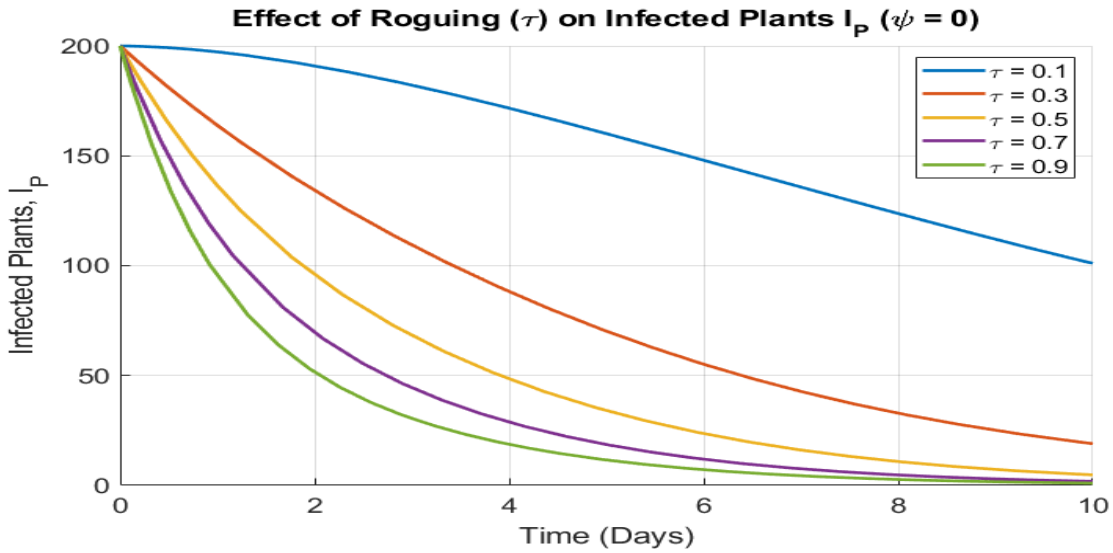

Figure 7: Effects of roguing rates on the Infected sesame plants (I_p).

Figure 7 Shows the dynamics of infected sesame plants (I_p) under varying roguing rates τ with $\nu = 0$ (no additional vector mortality) during the first 10 days following the observation of phyllody symptoms. As tau increases from 0.1 to 0.9, the infected plant population declines more rapidly, indicating that higher roguing rates are effective at reducing the infected plant population. Higher roguing rates (τ) significantly speed the decline of infected sesame plants, demonstrating roguing effectiveness in disease control even without additional vector mortality ($\nu = 0$). This accentuates the importance of timely roguing of infected plants to manage phyllody disease in sesame.

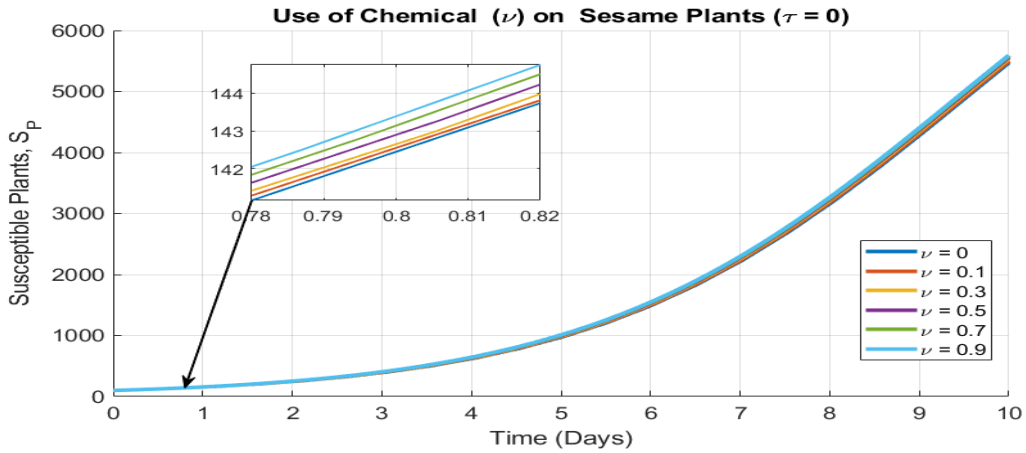

Figure 8: Effects of the use of chemicals on the susceptible plants.

Figure 8 shows that chemical application produces an exponential rise in the susceptible sesame plant population (S_P) in the first 10 days following the onset of phyllody symptoms. A higher nu reduces the number of vectors able to transmit phyllody, lowering infection pressure on the plants. The zoom near $t = 0.8$ years highlights early subtle differences, with higher nu yielding a slightly larger S_P even at the initial stage. Overall, increasing nu through chemical application helps maintain a larger healthy susceptible population by reducing the rate at which susceptible plants become infected.

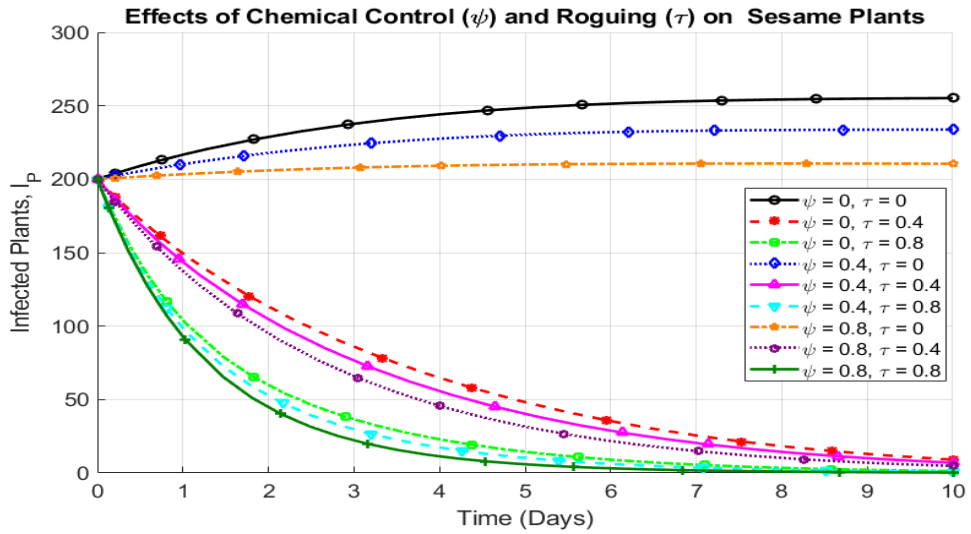

Figure 9: Effects of chemical control efficacy (ψ) and roguing rate (τ) on the infected sesame plant population (I_P) over three years

Figure 9 shows infected sesame plants (I_P) over 10 days for different chemical control (ψ) and roguing (τ) settings. Roguing alone reduces infections substantially ($\tau = 0$) to τ = 0.8
drives a rapid drop toward near zero by approximately day 5, while τ = 0.4 declines more slowly, with no roguing ($\tau = 0$) infections grow. Chemical control alone substantially ($\tau = 0$) has limited effect: even at $\psi = 0.8$ the curve is nearly flat and remains high, with ψ = 0.4 or 0 showing clear increases. Combining the two gives the steepest and most sustained declines. In addition, ψ = 0.8 with $\tau = 0.8$ is fastest, followed by ψ = 0.4 with τ = 0.8, then ψ = 0.8 with τ = 0.4. Overall, higher tau consistently dominates the dynamics, while ψ mainly shifts curves downward but is insufficient without roguing, together they produce the strongest reduction in I_P . Thus, this combination strategy provides the most effective approach for managing Phyllody disease in sesame by rapidly lowering infection burden and maintaining low levels of infected plants over time.

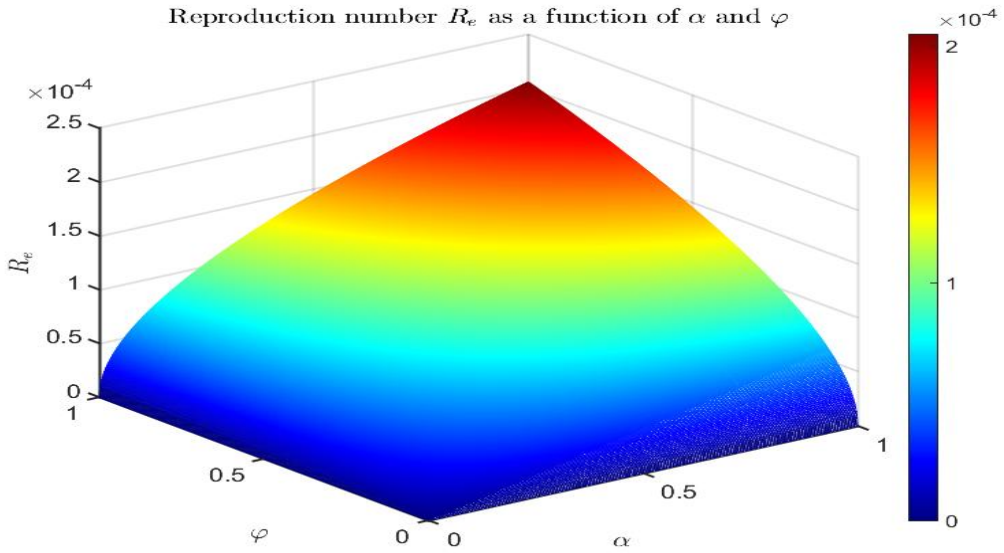

Figure 10: Variation of the effective reproduction number (R_e) with transmission rates from vectors to plants (α) and from plants to vectors (φ).

From Figure 10 it can be observed that increasing the transmission rates from vectors to plants (α) and from plants to vectors (φ) raises the effective reproduction number (R_e), with the highest R_e when both are high. Reducing either parameter lowers R_e, highlighting the effectiveness of integrated management strategies targeting both vector control (reducing α) and roguing of infected plants (reducing φ) to prevent Phyllody disease establishment and persistence

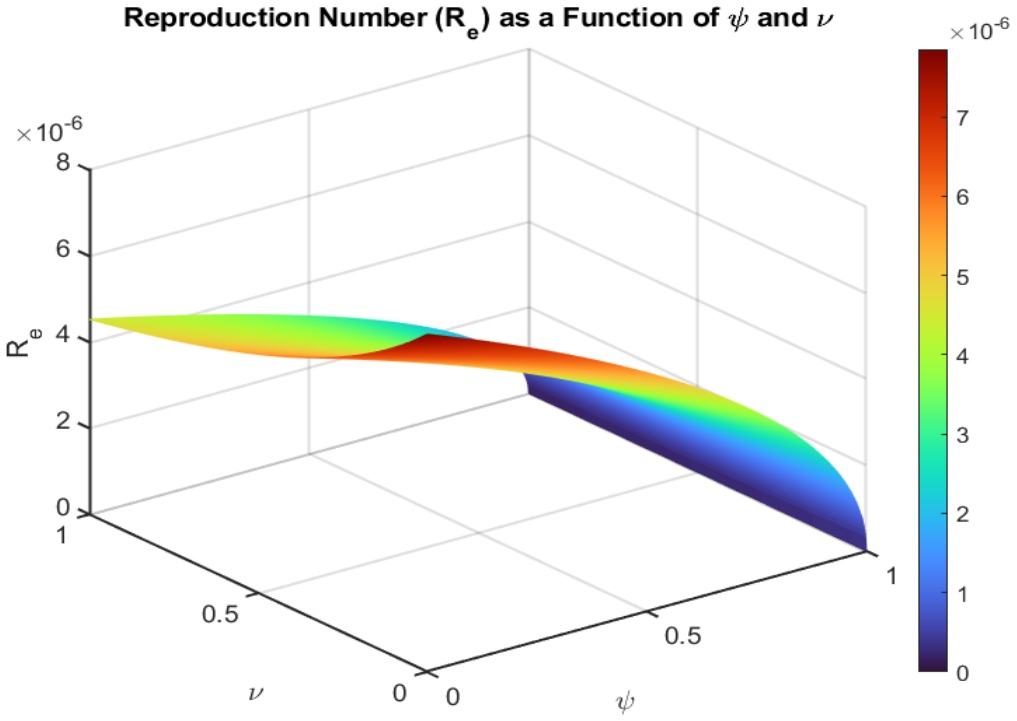

Figure 11: Effects of biological and chemical control strategies on the Effective reproduction number.

Figure 11 shows that increasing chemical control efficacy (ψ) and additional vector mortality (ν) both reduce the effective reproduction number (R_e) for Phyllody disease. Higher ψ lowers transmission from infected vectors to plants, while higher ν reduces vector lifespan and their capacity to transmit the pathogen. The lowest R_e values occur when both strategies are applied together, demonstrating that integrated use of chemical and biological controls is most effective in reducing R_e below threshold levels necessary for controlling or eliminating Phyllody disease in sesame fields.

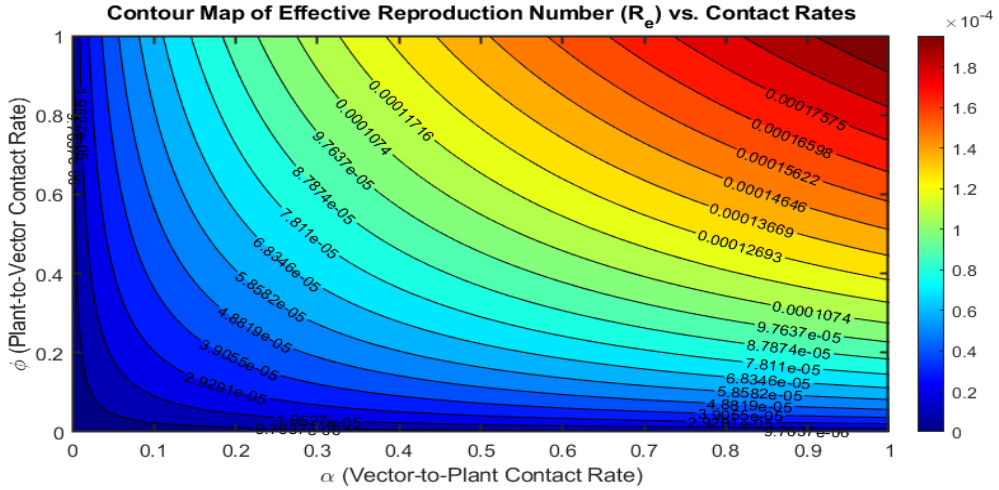

Figure 12 Contour map of the effective reproduction number (R_e) as a function of the vector-to-plant contact rate (α) and the plant-to-vector contact rate (φ).

Figure 12 shows that the effective reproduction number (R_e) increases with higher vector-to-plant (α) and plant-to-vector (φ) contact rates, indicating a greater potential for Phyllody disease spread under high transmission conditions. The labeled contours allow direct interpretation of R_e values across parameter combinations, demonstrating that lowering either α, φ, or both is effective in reducing R_e below critical thresholds for controlling the disease in sesame cultivation.

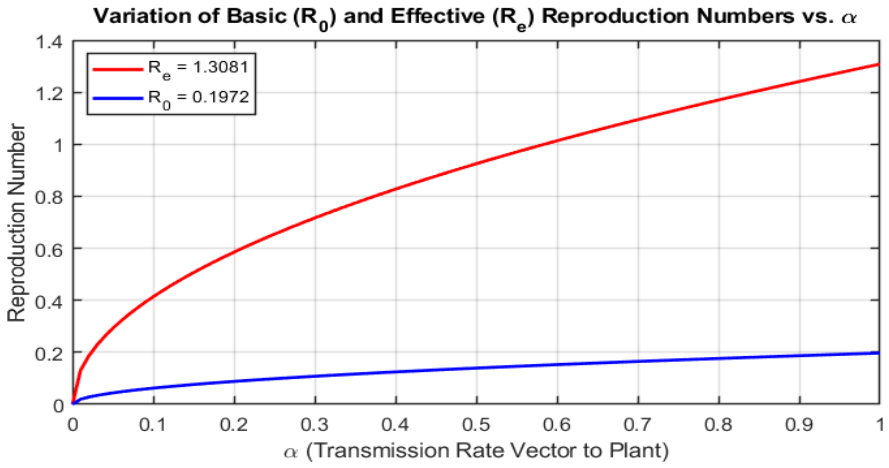

Figure 13: Variation of the Basic reproduction number and Effective reproduction number on the transmission rate of phytoplasma from the infected vector to susceptible plant.

Figure 13 illustrates the variation of the basic reproduction number (R_0) and effective reproduction number (R_e) as the transmission rate from infected vectors to susceptible plants (α) increases. At $\alpha = 1$, the calibration ensures that $R_0 = 0.1972$ and $R_e = 1.3081$, demonstrating the substantial reduction in transmission potential achieved through interventions such as chemical control and roguing. While R_0 increases with higher α, indicating greater potential for disease spread without interventions, R_e remains much lower across all αvalues under intervention, confirming the effectiveness of combined strategies in reducing Phyllody disease transmission in sesame fields.

Discussion

This study formulates and analyzes a sesame–phyllody transmission model with multiple controls. Results show that roguing (τ) alone produces a sharper short-horizon reduction in infected plants than chemical control (ψ) alone, while the combined deployment of roguing and chemical control achieves the fastest and most sustained decline in infections. These patterns align with modeling and field-guided evidence that prioritizes roguing or couples it with vector suppression (Qiu et al., 2021; Chapwanya and Dumont, 2021, Boopathi et al. 2023). The comparatively modest short-term impact of chemical control used in isolation departs from reports of stronger insecticide performance in some settings (Reddy et al. 2019, Singh et al. 2022), plausibly due to timing of application, coverage heterogeneity, or emerging resistance not captured by the present framework. Biological/cultural measures contribute additional, though slower-onset, gains—stabilizing trajectories and supporting sustained reductions when integrated with roguing and chemical control.

For example, Figures 4–13 summarise the control effects. In particular, Figures 4, 5, 6, and 8 show that biological and chemical interventions markedly suppress phyllody, consistent with reports that integrated seed treatments plus timely foliar sprays (e.g., imidacloprid followed by insecticide applications) reduce disease relative to unsprayed controls, with all tested packages outperforming controls (Shamaki et al. 2021, Sharma et al. 2023). More broadly, these findings accord with recent trials and reviews showing that vector-focused chemicals, complemented by bio/organic measures, effectively manage sesame phyllody (Qiu et al. 2021, Chapwanya and Dumont 2021, Collins and Duffy 2022, Gupta et al. 2023, Lukurugu et al. 2023, Chouksey et al. 2025). Further, higher chemical efficacy (ψ) and additional vector mortality (ν) both depress R_e, and the joint use of these measures performs best. This is consistent with integrated management perspectives and awareness style interventions that curtail contact and infectious exposure (Al Basir and Blyuss 2018, Boopathi et al. 2023, Yadav et al. 2023, Gupta et al. 2018).

In addition, our results in Figures 7 and 9 indicate that roguing symptomatic plants substantially suppresses phyllody, reducing infections and slowing transmission even when applied alone. When combined with vector control, it produces faster and larger declines in both infected plants and vector abundance, strengthening overall management. These findings accord with prior modelling and field-based analyses (Reddy et al. 2019, Al Basir et al. 2020, Ransingh et al. 2021, Gupta et al. 2023).

Moreover, the findings with contours analyses in Figures 10–12 show that the transmission rates φ (plant-to-vector acquisition) and α (vector-to-plant inoculation) strongly shape the effective reproduction number R_e. Increases in either parameter elevate R_e, whereas reductions lower it. These patterns are consistent with next-generation matrix analyses for vector–plant pathosystems (Jones 2007, Anguelov et al. 2012, Van den Bosch and Jeger 2017, Coronel et al. 2023).

Furthermore, our results in Figure 13 shows that higher vector to plant transmission increases (R_e). With controls ($\psi \neq 0, \tau \neq 0, \nu \neq 0$), R_e drops and stays below the baseline (R_0) ($\psi = \tau = \nu = 0$). This aligns with sensitivity-driven results in vector-borne systems that highlight transmission pathways as dominant levers (van den Driessche and Watmough, 2002; Chitnis et al. 2008; Shi et al. 2014, Van den Bosch and Jeger 2017, Al Basir et al. 2018, Anggriani et al. 2018, Al Basir et al. 2020, Qiu et al. 2021, Singh et al. 2022, Boopathi et al. 2023). Also, the calibration illustrates that as α increases, R_0 rises while R_e remains much lower under intervention, echoing classical reproduction-number theory and

stability insights (Castillo-Chavez and Song, 2004; Castillo-Chavez, Feng and Huang, 2002; LaSalle, 1976).

Some improvements are needed, as our study relies on a deterministic, well-mixed modeling framework and omits climate or seasonality and host–vector heterogeneity that can influence outcomes (Baath et al. 2022, Collins and Duffy 2022). The data used are illustrative rather than fully realistic, which may limit generalizability; nevertheless, they provide insight into the problem structure and can be replaced with field observations to obtain more plausible, site-specific estimates. Even so, the model has helped us assess the impact of multiple control strategies on the spread of phyllody disease in sesame.

Conclusion

In this study we developed and analysed a nonlinear deterministic transmission model for sesame phyllody, capturing interactions between sesame plants and the leafhopper vector population. The model was used to assess how different management strategies alter disease dynamics in the crop. We examined three forms of control: (i) biological and cultural practices (such as crop rotation, use of clean seed, field sanitation and timely planting), (ii) roguing (removal of symptomatic plants, τ), and (iii) chemical/vector control. The simulation results indicate that these interventions can substantially reduce both infected plants and infected vectors over time, and that integrated control produces the strongest and most sustained suppression of phyllody. Specifically, rapid removal of infected plants limits onward transmission from diseased plants to vectors, while vector-focused measures further reduce infection pressure on healthy plants. However, our results also show that no single intervention is universally sufficient: roguing applied in isolation does not fully prevent continued infection in the vector population, and chemical control alone may have limited short-term effect if application is not well timed. These findings imply that phyllody management should be viewed as an integrated, seasonally planned process rather than a one-off action. We therefore recommend that farmers and extension officers prioritise early detection and prompt roguing of symptomatic plants, combined with appropriate vector suppression and good agronomic practices (field sanitation, removal of volunteer hosts, timely planting, and use of healthy seed material). For policy and advisory agencies, the model supports promoting coordinated, multi-component management guidelines rather than relying solely on spraying, especially in areas and seasons with high vector pressure.

Funding

The preparation of this manuscript was not supported by any funding.

Declaration of competing of Interests

The authors declare no conflicts of interest.

Data availability

Data were gathered from various sources in the literature and are cited throughout the manuscript.

Acknowledgments

We are grateful to the Dar es Salaam University College of Education and the Department of Mathematics at the University of Dar es Salaam for providing continuous internet access and other library resources.

References

Abdipour M, Ramazani SH, Younessi-Hmazekhanlu M, Niazian M 2018 Modeling oil content of sesame (Sesamum indicum L) using artificial neural network and multiple linear regression approaches. *J. Am. Oil Chem. Soc*. *Mar* 95(3):283-97.

Ahmed E A, Farrag AA, Kheder AA, and Shaaban A 2022 Effect of phytoplasma associated with sesame phyllody on ultrastructural modification, physio-biochemical traits, productivity and oil quality. *Plants.* 11(4): 477.

Al Basir F, Blyuss KB and Ray S 2018 Modelling the effects of awareness-based interventions to control the mosaic disease of *Jatropha curcas*. *Eco. Complex*. 36:92-100. https://doi.org/10.1016/j.ecocom.2018.07.002

Alemneh HT, Makinde OD and Theuri DM 2019 Mathematical modelling of MSV pathogen interaction with pest invasion on maize plant. *Global J. Pure Appl. Math.* 15(1):55-79.

Anggriani N, Ndii MZ, Arumi D, Istifadah N and Supriatna AK 2018 Mathematical model for plant disease dynamics with curative and preventive treatments. *In AIP Conference Proceedings*. https://doi.org/10.1063/1.5079196

Anguelov R, Dumont Y and Lubuma JMS 2012 Mathematical modeling of sterile insect technology for control of Anopheles mosquito. *Comput. Math. Appl*. 64(3): 374 – 389. https://doi.org/10.1016/j.camwa.2012.02.068.

Baath GS, Kakani VG, Northup BK, Gowda PH, Rocatel AC and Singh H 2022 Quantifying and modelling the influence of temperature on growth and reproductive development of sesame. *J. Plant Growth Regul*. https://doi.org/10.1007/s00344 – 022–10648–8

Boopathi T, Sujatha M, Prasad M, Duraimurugan P, Sakthivel K, Ramya KT and Rathnakumar AL 2023 Phytoplasma on sesame: etiology, insect vectors, molecular characterization, transmission and integrated management. *Curr. Sci. (*00113891). 125(4). https//doi.10.18520/cs/v125/i4/383-391

Bounkaicha C and Allali K 2024 Modelling disease spread with spatio-temporal fractional derivative equations and saturated incidence rate. *MESE.* 10(1):259-71. 10.1007/s40808-023–01773–8.

Castillo-Chavez C and Song B 2004 Dynamical models of tuberculosis and their applications. *Math. Biosci. Eng.* Jul 1;1(2):361-404. 10.3934/mbe.2004.1.361

Castillo-Chavez C, Feng Z and Huang W 2002 On the Computation of R (o) and Its Role on Global Stability. 10.1007/978-1-4613-0065–6–13.

Chapwanya M and Dumont Y 2021 Application of mathematical epidemiology to crop vector-borne diseases: The cassava mosaic virus disease case. *IDOP.* 57-95. 10.1007/978-3-030-50826–5–4.

Chitnis N, Hyman JM and Cushing JM 2008 Determining important parameters in the spread of malaria through the sensitivity analysis of a mathematical model. *Bull.*

Math. Biol. 70:1272-96. 10.1007/s11538-008-9299-0 10.1007/s11538-008-9322-6

Chouksey V, Gupta KN and Vishwakarma AK 2025 Management of phyllody of sesame. *TSBAS.*

Chuma FM and Ngailo EK 2024 Mathematical analysis of campylobacteriosis disease model in human with saturated incidence rate and treatment. *Math. Open.* 3:2350011. 10.1142/S2811007223500116.

Chuma FM and Mwanga GG 2020 Bifurcation Analysis of Newcastle Disease Eco-Epidemiological Model in the Presence of Vaccination: A Case of the Backyard Chicken. *J. Educ. Humani Sci.* 9(2): https://doi.org/10.56279/jhss.v9i2.52

Chuma FM and Mwanga GG 2019 Stability analysis of equilibrium points of Newcastle disease model of village chicken in the presence of wild birds reservoir. International J. *Math. Sci. Comput.* 5(2):1-8. 10.5815/ijmsc.2019.02.01.

Collins OC and Duffy KJ 2022 A stochastic epidemic model for the dynamics and control of maize streak disease. *Acta Agric. Scand. B Soil Plant Sci.* 72(1):635-47. 10.1080/09064710.2022.2046491.

Coronel A Huancas F and Berres S 2023 Study of an epidemiological model for plant virus diseases with periodic coefficients. *Appl. Sci.* 14(1): 399.

El-Mashharawi HQ and Abu-Naser SS 2019 An Expert System for Sesame Diseases Diagnosis Using CLIPS. *Int. J. Acad. Eng. Res.* 3(4):22-9.

Fantaye AK and Birhanu ZK 2023 Modeling and analysis for the transmission dynamics of cotton leaf curl virus using fractional order derivatives. *Heliyon.* Jun 1;**9**(6). 10.1016/j.heliyon.2022.e08997.

Gogoi SH, Kalita MK and Nath PD 2017 Biological characterization of sesamum phyllody disease in Assam, *India. J. Curr. Microbiol. Appl. Sci.* 6(11): 1862-1875.

Goswami NK, Olaniyi S, Abimbade SF and Chuma FM 2024 A mathematical model for investigating the effect of media awareness programs on the spread of COVID-19 with optimal control. *Healthcare Analytics*. Jun 1; 5:100300. 10.1016/j.health.2024.100300.

Gupta KN, Naik KR and Bisen R 2018 Status of sesame diseases and their integrated management using indigenous practices. *Int. J. Chem. Stud* 6(2):1945-52.

Gupta KN, Yashowardhan S, Panday AK and Bisen R 2022 Sesame phyllody disease: Its symptomatology, etiology, and transmission in Pakistani. 10.22271/tpi.2022.v11.i12b.11.

Jones JH 2007 Notes on R0. *Calif: Dept. Anthropol. Sci*. 323, pp.1-19.

Khan MA, Khan Y and Islam S 2018 Complex dynamics of an SEIR epidemic model with saturated incidence rate and treatment. *Phys. A: Stat. Mech. Appl*. 493:210-27. https://doi.org/10.1016/j.physa.2017.10.038.

Ikten C, Ustun R, Catal M, Yol E, and Uzun B 2016 Multiplex real-time qPCR assay forsimultaneous and sensitive detection of phytoplasmas in sesame plants and insect vectors. *PLoS One* 11(5): e0155891.

Kolte SJ 2018 Diseases of annual edible oilseed crops: Volume II: rapeseed-mustard and sesame diseases. *CRC press.* an 18. DOIhttps://doi.org/10.1201/9781351071437.

Kumari S, Prameela HA and Hurakadli MS 2016 Chemical management of China aster (Callistephus chinensis L Nees.) phyllody disease. *J. Pure Appl. Microbiol*. 10(4):2871-4. 10.22207/jpam.10.4.49

Kumar P, Baleanu D, Erturk VS, Inc M and Govindaraj V 2022 A delayed plant disease moel with Caputo fractional derivatives. *Adv. Contin. Discrete Models.* (1):11. https://doi.org/10.1186/s13662-022-03684-x

LaSalle JP 1976 Stability theory and invariance principles. In Dynamical systems 1976 Jan 1 (pp. 211-222). *Acad. Press.*

Liana YA and Chuma FM 2023 Mathematical modelling of giardiasis transmission dynamics with control strategies in the presence of carriers. *J. Appl. Math.* (1):1562207. https://doi.org/10.1155/2023/1562207

Lukurugu GA, Nzunda J, Kidunda BR, Chilala R, Ngamba ZS, Minja A and Kapinga FA. 2023 Sesame production constraints, variety traits preference in the Southeastern Tanzania: Implication for genetic improvement. *J. Agric. Food Res*. 14:100665. https://doi.org/10.1016/j.jafr.2023.100665

Mbuthia FK and Chepkwony I 2019 Mathematical modelling of tungiasis disease dynamics incorporating hygiene as a control strategy. *J. Adv. Math. Comput. SciMar*. 33(5):1-8. https://doi.org/10.9734/jamcs/2019/v33i530190

Melese AS, Makinde OD and Obsu LL 2022 Mathematical modelling and analysis of coffee berry disease dynamics on a coffee farm. *Math. Biosci. Eng.* 19(7):7349-73. https://doi.org/10.3934/mbe.2022347

Mrope MF, Filmon AM and Nyerere N 2025a Mathematical modeling of powdery mildew disease in cashew plants with optimal control and cost-effectiveness analysis, *Modeling Earth Systems and Environment,* 11(4): 300.

Mrope MF, Nyerere N and Filmon AM 2025b Modeling the transmission dynamics of powderly mildew disease in cashew plants, Modeling Earth Systems and Environment, 11(3): 182.

Mushayabasa S, Marijani T, Masocha M 2017 Dynamical analysis and control strategies in modeling anthrax. *Comp. Appl. Math*. *Sep*. 36(3):1333-48. https://doi.org/10.1007/s40314-016-0390-6

Naaly BZ, Marijani T, Isdory A and Ndendya JZ 2024 Mathematical modeling of the effects of vector control, treatment and mass awareness on the transmission dynamics of dengue, *Comput. Methods Program Biomed. Update*. 6: 100159. https://doi.org/10.1016/j.cmpbup.2024.100159

Olaniyi S, Lawal IA, Lebelo RS, Chuma FM, Abimbade SF 2025 Modelling and Optimal Control of Influenza Dynamics with Structured Populations Based on Education and Isolation. *Int. J. Anal. Appl.* Mar 31; 23:8. https://doi.org/10.28924/2291-8639-23-2025-81

Olaniyi S, Abimbade SF, Chuma FM, Adepoju OA and Falowo OD 2023 A fractional-order tuberculosis model with efficient and cost-effective optimal control interventions. *Decis. Anal. J.* Sep 1; 8:100324. 10.1016/j.dajour.2023.100324

Olaniyi S and Chuma FM 2023 Lyapunov stability and economic analysis of monkeypox dynamics with vertical transmission and vaccination. *Int. J. Appl. Comput. Math.* 9(5):85.

https://doi.org/10.1007/s40819-023-01572-w

Qiu G, Tang S and He M 2021 Analysis of a High-Dimensional Mathematical Model for Plant Virus Transmission with Continuous and Impulsive Roguing Control. *Discrete Dyn. Nat. Soc.* 2021(1):6177132.

Ramesh K, Ratnakumar P, Harisudan, Bhaskar C and Reddy AV 2019 Sesame (Sesamum indicum) in the rice fallow environment-a critical appraisal. *J. Oilseeds Res.* 36(4): 203-209.

Ransingh N, Khamari B, Adhikary NK 2021 Modern approaches for management of sesame diseases. In Innovative approaches in diagnosis and management of Crop Diseases. *Apple Academic Press*. (pp. 123-162).

Reddy TV, Prasad KH, Chalam M and Viswanath K 2019 Management of Leafhopper (Orosius albicintus) of sesamum with certain insecticides. *Andhra Pradesh J Agri. Sci*. **5**(3).

Santha Lakshmi Prasad M, Surya Prakash Reddy M, Duraimurugan P, Prasindhu K, Jawaharlal J, Ramya KT, Kumaraswamy HH, Sujatha M, Alivelu K, Sakthivel K and Boopathi T.Akhtar et al. 2009 Identification of resistance sources for sesame phyllody under epiphytotic conditions in India. *Genet. Resour. Crop Evol.* 72(2):2131-40.

Shamaki TA, Adesanya OA and Musa S 2021 Biological Control of Vector-Borne Viral Diseases in Solanaceous Vegetable Plants: Mathematical Modelling Approach. *CaJoST* 3(1):43-54.

Sharma JK, Lekha, Shekhawat HVS, Joshi N, Meena VK and Sharma K 2023 Management of sesame phyllody: a destructive disease of South-western Rajasthan.

Singh VB, Singh AK, Srivastava JN and Singh SK 2020 Important Diseases of *Sesamum* (*Sesamum indicum* L.) and Their Management. In Diseases of Field Crops Diagnosis and Management. Apple Academic Press. (pp. 259-285).

Shi R, Zhao H and Tang S 2014 Global dynamic analysis of a vector-borne plant disease model. *Adv. Differ. Equ.*1-6.

Singh Y, Gupta KN, Kharte S and Malempati SS 2022 Management of Sesame Phyllody disease through the insecticide in Madhya Pradesh. Ecology, Environment and Conservation. 28(4):286-9.

Stella IR, Srivastav AK and Ghosh M 2021 Modeling and analysis of vector-borne plant disease with two delays. *IOP Publishing*: Conference Series. May 1 (Vol. 1850, No. 1, p. 012125).

Texas A and M AgriLife 2007 Research and Extension Center at San Angelo. (January 29). *Sesame–production guide*.https://sanangelo.tamu.edu/agronomy/agronomy-publications/sesame-production-guide/

Vamshi J, Devi GU, Rao SC and Sridevi G 2018 Sesame phyllody disease: Symptomatology and disease incidence. *Int. J. Curr. Microbiol. App. Sci*;**7**(10):2422-37.

Van den Bosch F and Jeger MJ 2017 The basic reproduction number of vector-borne plant virus epidemics. Virus Res. 241: 196-202.

van den Driessche P and Watmough J 2002 Reproduction numbers and sub-threshold endemic equilibria for compartmental models of disease transmission. *Math. Biosci.* 180(1-2):29-48.

Verma ML, Naresh Mehta NM and Sangwan MS 2025 Fungal and bacterial diseases of sesame.

Vemana K, Rao GP, Kalita MK, Esmaeilzadeh-Hosseini SA, Azadvar M and Li Z 2023 Update on phytoplasma diseases associated with oil seed crops in Asia. In Phytoplasma diseases of major crops, trees, and weeds 2023. *Acad. Press*. (pp. 105-124). https://doi.10.1016/C2021-0-00254-6

Weintraub PG and Beanland L 2006 Insect vectors of phytoplasma. *Ann. Rev. Entomol.* 51(1): 91111. https://doi.10.1146/annurev.ento.51.110104.151039.

Yadav PD, Rathore GS, Choudhary S, Sharma RS and Meena R 2023 Management of Sesame Phyllody: A Destructive Disease of East-Central Rajasthan, India. *Int. J. Plant Soil Sci*. 35(23):182-8. https://journalijpss.com/index.php/IJPSS/article/view/4230